INSTITUTO POLITÉCNICO DE LISBOA

Instituto Superior de Engenharia de Lisboa
Escola Superior de Tecnologia da Saúde de Lisboa

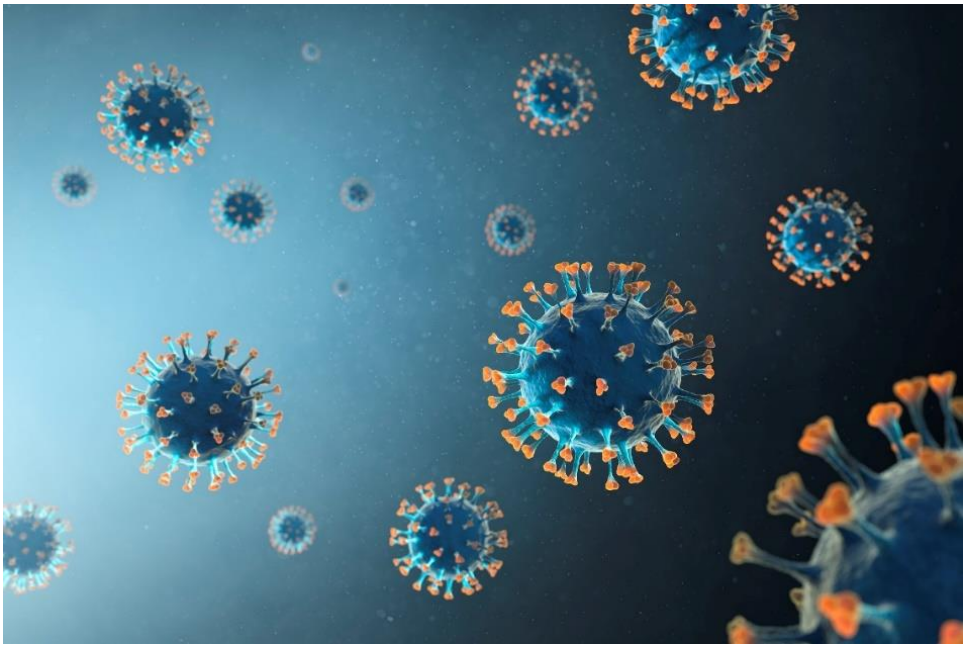

Discovery of Infection Biomarkers Based on Metabolomics

Tiago Francisco Rosa Domingues Alexandre

Thesis to obtain the Master's degree in **Biomedical Engineering**

Definitive Version

Supervisors

Cecília Ribeiro da Cruz Calado (ISEL)
Joana Silvestre (Hospital Lusíadas Lisboa, ISEL)
António Ricardo (Hospital Lusíadas Lisboa, ISEL)

November 2022

INSTITUTO POLITÉCNICO DE LISBOA

Instituto Superior de Engenharia de Lisboa
Escola Superior de Tecnologia da Saúde de Lisboa

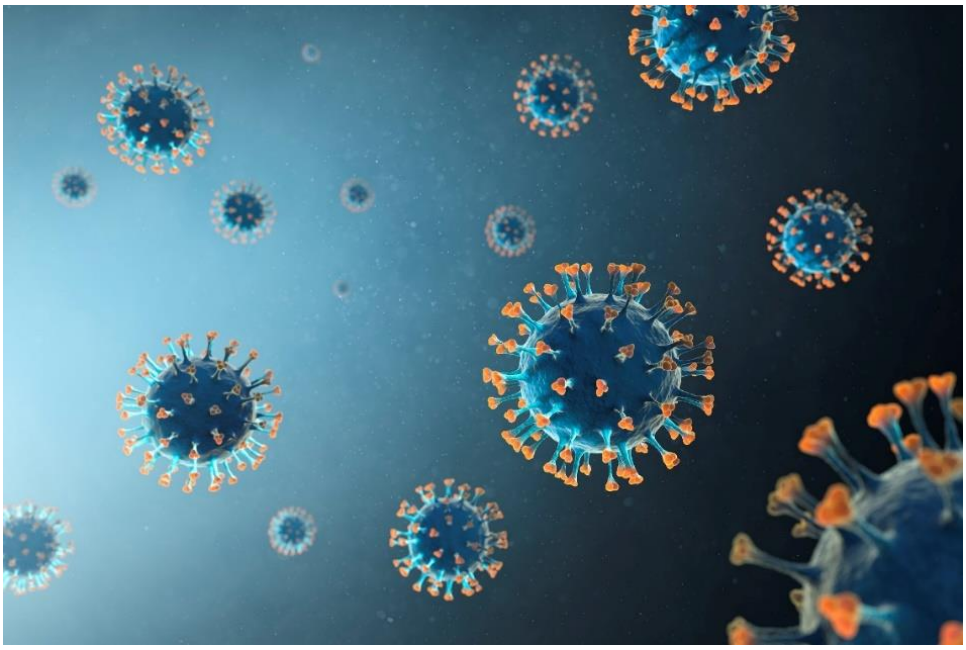

Discovery of Infection Biomarkers Based on Metabolomics

Tiago Francisco Rosa Domingues Alexandre

Thesis to obtain the Master's degree in **Biomedical Engineering**

Supervisors:

Cecília Ribeiro da Cruz Calado (ISEL)
Joana Silvestre (Hospital Lusíadas Lisboa, ISEL)
António Ricardo (Hospital Lusíadas Lisboa, ISEL)

Examination Committee:

Chairperson

Paulo Jorge Leitão Pessoa Guerreiro (ESTeSL)

Members of the committee

Cecília Ribeiro da Cruz Calado (ISEL)

Luís Filipe Nunes Bento (CHULC)

November 2022

Discovery of Infection Biomarkers Based on Metabolomics

Tiago Francisco Rosa Domingues Alexandre

This research was funded by project grant DSAIPA/DS/0117/2020 and PTDC/EQU-EQU/3708/2021, supported by Fundação para a Ciência e a Tecnologia, Portugal.

The present work was conducted in Instituto Politécnico de Lisboa and in the Engineering & Health Laboratory, that resulted from a collaboration protocol established between Universidade Católica Portuguesa and Instituto Politécnico de Lisboa.

Acknowledgments

I would like to formally thank Professor Cecilia Calado for allowing me to be integrated into the Engineering & Health Laboratory at ISEL, as well as the PREMO project. Initially, I was promised an idea of yours for my soon to be thesis project, and what came out from it, was bigger than what I ever imagined. I would also like to thank Joana Silvestre and António Ricardo for orienting me during this thesis.

An immense thank you to Luís Bento for guiding me through some rough roads and leading me on to make this thesis possible, providing me with all the data used in this project, as well as the knowledge I needed at times to fully understand my hardships.

I would like to give a shout out for my lab mates, which made every day either fun or a little less stressful. And so, Rubén, Cristiana, Tiago, Raquel, Diogo, thank you for the laughs and headaches.

Leaving my family at the end of my acknowledgements merely means to show how much of a foundation for me to complete this thesis they represent. Being there to show concern and give a hand when things seem troubling is one of the most powerful tools for anyone to go through a challenge. And my family allows me to be inspired, and resilient towards my goals, to achieve the very best of who I can be.

Finally, without Sofia, every day would feel heavier, and every sky would appear as cloudy. She has been my ray of sunlight for the complete duration of this project, motivating me with the amazing future I aspire to achieve, seeing this as just another rock for me to climb. And even when I feared I would fall, she would show me she would be there to be my safety net. And for that, I thank you all.

Resumo

Enquadramento e objetivos: Pacientes críticos de COVID-19 são regularmente admitidos nos cuidados intensivos com diversas complicações, necessitando de tratamentos mais invasivos. Para além disso, os pacientes estão expostos a uma ameaça iminente de infeções durante a sua estadia hospitalar. Estas infeções podem levar ao agravamento do estado de saúde do paciente, e tendo em conta o estado atual do paciente COVID-19 critico, pode ser fatal caso não seja devidamente identificada a presença de infeção e iniciado o tratamento mais adequado. Nesta tese, o foco foi dividido em dois objetivos: determinar uma metodologia capaz de identificar mais rapidamente um estado ativo de bacteremia no paciente COVID-19 critico; e identificar a tipologia de Gram da bactéria que originou a bacteremia.

Métodos: Recorrendo-se ao método do espectrometria de FTIR, e testes Principal Component Analysis (PCA), Hierarchical Cluster Analysis (HCA) e Linear Discriminant analysis (PCA-LDA), para realizar analise discriminante de uma amostra com objetivo de testar o método mais eficaz na discriminação entre pacientes com bacteremia (n=48) e pacientes sem bacteremia (n=54), e entre amostras com bactéria Gram-positiva (n=28) e bactéria Gram-negativa (n=20).

Resultados: Através dos testes PCA e HCA não foi possível obter uma discriminação fidedigna nem entre amostras com e sem bacteremia, nem entre bactérias Gram-positivas e Gram-Negativas. A vasta variabilidade associada a amostras biológicas pode justificar este resultado. PCA-LDA, possibilitou resultados de 75% de eficácia na discriminação entre amostras de bacteremia e sem bacteremia, e uma eficácia de 85% na discriminação entre amostras com bactérias Gram-positivas e bactérias Gram-negativas.

Conclusão: Os resultados apontam para a possibilidade da utilização da análise de espetro de espetrometria FTIR como um método apelador para o diagnóstico de bacteremia e classificação do tipo de bactéria, de uma forma simples e rápida, permitindo uma gestão mais eficiente deste tipo de pacientes críticos.

Palavras-chave: Biomarcadores, infeção, bacteremia, COVID-19, FTIR, espetroscopia

Abstract

Background and Goals: Critical COVID-19 patients are regularly admitted with diverse complications leading to Intensive care unit (ICU) admission. Besides these patients are constantly exposed to the threat of infection during their hospital stay. These infections may lead to the worsening of the patient's health and considering the already debilitated state of the critical COVID-19 patient, may be fatal if the infection agent isn't correctly identified and treated within the most appropriate timing upon diagnosis. In this thesis, the focus of the study was divided into two main sections: to determine a method capable of faster identification of bacteremia in the critical COVID-19 patient; and to identify Gram bacteria causing the bacteremia.

Methodology: Utilizing the FTIR spectroscopy method, and spectra principal component analysis (PCA), hierarchical cluster analyses (HCA) and linear discrimination analyses (PCA-LDA) applied to serum samples of bacteremia patients (n=48), non-bacteremia patients (n=54), and samples with Gram-positive (n=28) from Gram-negative (n=20) bacteria. Diverse spectra pre-processing methods were evaluated.

Results and discussion: Spectra PCA and HCA, did not shown samples patterns enabling to separate between bacteremia and non-bacteremia samples, nor between Gram-positives and Gram-negative bacteria. The high variability associated with these patients may justify the obtained result. Spectra PCA-LDA enabled discrimination accuracy results of 75% between bacteremia and non-bacteremia samples, and of 85% for discrimination between Gram-positive and Gram-negative bacterial samples.

Final remarks: The results point to the potential of FTIR spectroscopy as a very appealing method to conduct the diagnosis of bacteremia and the classification of the type of bacteria, in a simple and rapid mode, enabling a more efficient management of this type of critical patients.

Key words: Biomarkers, infection, bacteremia, COVIID-19, FTIR spectroscopy

Table of Contents

List of figures

List of tables

List of abbreviations

ACE2 - Angiotensin-Converting Enzyme II
ARDS - Acute respiratory distress syndrome
BMI - Body mass index
CAUTI - Catheter-associated urinary tract infection
CD64 - Cluster of differentiation 64
CLABSI - Central line-associated bloodstream infections
COVID-19 - Coronavirus disease 2019
CRP - C-Reactive protein
CVC - Central venous catheters
CVCBSI - Central venous catheter bloodstream infection
ECMO - Extracorporeal membrane oxygenation
FGR - Functional group region
FIR - Far-infrared
FTIR - Fourier-transform infrared
GI - Gastrointestinal infection
HAI - Hospital Acquired Infection
HCA - Hierarchical cluster analyses
HFO - High flow oxygen
ICU - Intensive care unit
IL-6 - Interleukin 6
IMV - Invasive mechanical ventilation
LDA - Linear discriminant analyses
MERS - Middle east respiratory syndrome
MIR - Mid-infrared
NIPALS - Non-linear iterative partial least squares
NIR - Near-infrared
PCA - Principal component analyses
PCT - Procalcitonin
PREMO - Predictive models of COVID-19 outcomes for Higher Risk Patients Towards a Precision medicine
PMN - Polymorphonuclear Neutrophils
SARS - Severe acute respiratory syndrome
SSI - Surgical site infection
SVD - Singular Value Decomposition
VAP - Ventilator associated pneumonia
VOC **-** Variants of concern
VOI **-** Variants of interest
WHO - World health organization

1 Thesis objectives and Work Structure

Since the first discovery and development of what would be the biggest infectious outbreak of the 21st Century, COVID-19 continues to damage health systems across the world, leading to the worsening of health conditions. COVID-19 has been proven to display a harsher prognostic in the elderly and people with other comorbidities, such has hypertension, diabetes, cancer, or respiratory related illnesses [1]. The individuals that display a higher necessity for a more rigorous and constant treatment, are inserted into intensive care units. The patients that are directed into the intensive care unit tend to have a longer hospital stay, a significant increase in the incidence of respiratory failure and acute respiratory distress syndrome (ARDS), thus ending in a higher mortality rate [2].

One of the risk factors of stays in the ICU is related to nosocomial infections. Hospital-Acquired Infections (HAI) are extremely common, even more so in countries with higher poverty rates [3]. If an individual with a weaker immune system gets infected such as most ICU patients, it could be enough to increase the likelihood of death. Bacteria are the culprit for the majority of HAI. They're the main responsible for pneumonia cases, the most common HAI in hospital settings, and the single largest infectious cause of death in children worldwide (22% in children aged 1 to 5) [4]. The deadliest form of infection comes from central line-associated bloodstream infections, (CLABSI), with a death incidence rate ranging from 12% to 25%. It consists of infection in the blood, as a consequence of using catheters to transfer liquids and medicine to the central line [5].

Therefore, identification of bacteria responsible for co-infection in severe COVID-19 cases in the ICU is crucial and needs to be immediately treated with the correct antibiotic therapy, to increase the chances of survival.

Being that COVID-19 patients in the ICU are at a higher risk to develop bacteremia due to being associated with prolonged hospital stays, a weakened immune system, and higher risk for bacterial contamination, this thesis aims to:

- Achieve a faster, yet reliable, methodology for identification of bacteria causing bacteremia in critical COVID-19 patients in the ICU, by use of Fourier-transform infrared spectroscopy (FTIR);
- Identify the Gram strain of bacteria responsible for bacteremia, to correctly start antibiotic therapies;

- Be able to consequently reduce the need for exacerbated use of antibiotics prior to bacteria identification, avoiding the worsening of the patient's condition and helping in the regression of antibiotic-resistant bacteria.

The thesis is organized into 5 chapters:

- **Chapter 1**: Objectives
- **Chapter 2**: Literature Review
- **Chapter 3**: Methodology
- **Chapter 4**: Results and Discussion
- **Chapter 5** Conclusions and Future developments

To initiate the thesis, an initial extensive literature review was conducted to acquire full information of the SARS-CoV-2 virus, how it functions and how it reacts and interacts with the human organism to establish infection, such as what consequences it brings as it worsens, in ICU COVID-19 patients. Followed by an analysis on how bacteremia can enter and attack the weakened health of a critic patient admitted to ICU, and the way it can be identified through FTIR spectroscopy analysis, for a fast identification of the bacteria and its gram strain to identify the correct antibiotic therapy to follow for proper treatment.

The thesis also went deep into what is the FTIR spectroscopy workflow and how it operates, what it detects and how it has been previously used for similar studies, revealing its diagnostic capabilities. In the end, we'll be able to establish how exactly FTIR spectroscopy can be a powerful weapon in the diagnosis of bacteremia in COVID-19 patients in the ICU.

The methodology section goes over the various procedures performed in the development of the thesis, to study every possible variable that was relevant, such as demographic, clinical, and statistical related variables. In the end, it enabled the definition of the study sample used. The results obtained with this study sample, were presented, and discussed in union, to reach conclusions on how the effects of FTIR spectroscopy related diagnosis of bacteremia on ICU COVID-19 patients can be impactful and effective.

Utilizing the statistical analysis software Unscrambler™, it was possible to analyze significant differences between COVID-19 with bacteremia patients and the control group composed of COVID-19 clear of bacteremia. Furthermore, a trial on identification of gram strain was also performed, to observe if FTIR spectroscopy was a capable work method in defining the best antibiotic therapy for the specific bacteria detected in the patients, versus the standard laboratory method, that include culture growth and gram staining.

2 Literature review

2.1 Origin and evolution of the SARS-CoV-2 pandemic

In late 2019, a massive outbreak of pneumonia cases was seemingly occurring in Wuhan, China. This led to an uprising state of alertness, since it appeared to be related to a possible virus spreading in the city's population. The origin of the virus was being associated with the Wuhan Huanan Seafood Wholesale Market, since a vast majority of initial cases, were its active workers. It was feared that the immense availability of aquatic food products and farmed wild animals under the environment of a crowded market, would possibly originate a human-animal interface, capable of passing a virus to human hosts. The virus was given the name of SARS-CoV-2.

Several other cases were later reported to have not been in association with the market, leading on to doubt of the certainty that the market was the correct epicenter of the disease. It was later determined that upon isolating and sequencing the virus, It belonged to the *Coronaviridae* family, displaying similarities to the 2002-2004 coronavirus responsible for the SARS pandemic, as well as a 96% homology with a sequence of a coronavirus strain (RaTG13) identified in a horseshoe bat sample, thus being the closest known sequence to the recent SARS-CoV-2 [6].

On the 11th of February 2020, the International Committee on Taxonomy of Viruses declared the name for the newfound virus would be "Severe Acute Respiratory Syndrome Coronavirus 2" (SARS-CoV-2), with the WHO announcing the disease to follow the name of COVID-19 [7]. As the disease started to spread at an alarming rate in other major countries, the WHO characterized COVID-19 as a pandemic [8].

Various safety procedures were initiated to contain new infections and hospital admissions. The lack of a studied form of effective treatment, made several affected nations create strategies involving nationwide lockdowns, quarantine, regular testing, and total shutdown of international borders, to reduce international travel of the virus [9]. As time passed, there would be noticeable improvement on new outbreaks, with Australia, for example, reducing cases by 91,7% upon shutdown [10]. But although diagnosed infections were decreasing, the prevention methods led to multiple countries suffering with an increasing unemployment growth, the fall of millions of businesses and the increase in worldwide poverty, hunger and malnutrition [11].

With the advancement of the virus infectivity, and human-to-human spread, several mutations in the virus led to development of various strains of this infectious virus. These variations can lead to higher disease severity, spread capability, and how It reacts to treatments such as vaccines. These can be separated into variants of interest (VOI) and variants of concern (VOC).

What distinguishes a VOI from a VOC, is its severity and probable effect on the global population. VOC consists of a line-up of variants labeled by the WHO as Alpha (B.1.1.7), Beta (B.1.351), Gamma (P.1) and Delta (B.1.617.2). These were individually studied and monitored, to ensure proper prevention measures worldwide. The variant Alpha was the first on to be identified on the 18th of December.

A VOI represents any variant that displays mutations suspected or known to cause how the virus performs in its infection capability or is widely spread. These are possible VOCs, if for example, the variant is confirmed to infect more easily, leads to more severe health complications, and endangers the use of known treatments as they become ineffective. Currently VOCs include the current Omicron variant which was documented for the first time in multiple countries in November of 2021. Studies showed that, whilst the Omicron variant displayed a high infectability rate and an increased immune evasion, its lower severity lead to a accentuated decrease of hospitalizations and deaths [12,13].

Multiple major pharmaceutical companies began investing in creating the most effective vaccine to increase general immunity, alleviating the exacerbated pressure on hospital admissions. Data regarding the viral genome and new findings of potential therapies began to arise as more of the virus investigated, by case studying and genome sequencing. The formulation of a vaccine is, on average, extremely time-consuming, going through multiple phases to ensure proper research and clinical trials, for a safe final product to be distributed to the masses, as can be shown on **Figure *2.1.1***.

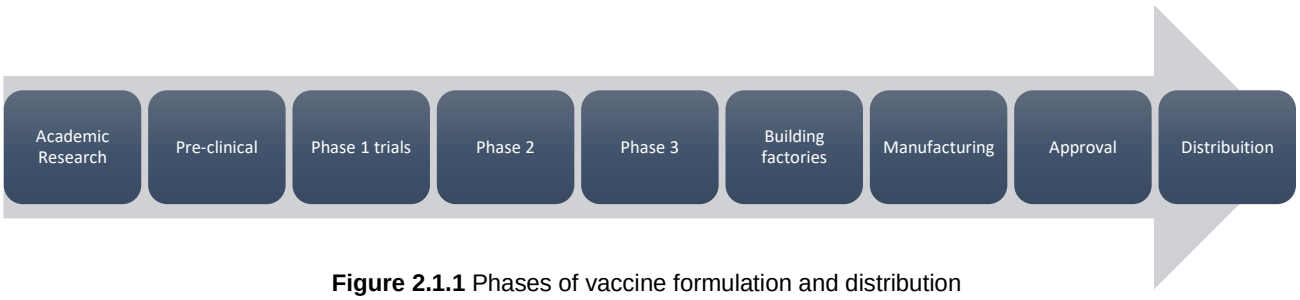

Figure 2.1.1 Phases of vaccine formulation and distribution

However, as more and more pressure for vaccine creation was being put on these major pharmaceutical companies, such as Pfizer, Moderna and Janssen, trial phases were performed at a larger scale than what would normally occur, performing them simultaneously to get final finished product on schedule [14]. In 2021, vaccines start to be administered to the general population, lowering infection and death rates significantly [15,16].

Since the initial spread in Wuhan, China, SARS-CoV-2 reached all-round the globe, gaining infection and death rates of unimaginable rates. As of August 2022, worldwide cases have hit approximately 587 million and 6,4 million deaths, in total. Europe remains as the main region of virus spread (42%) whilst the Americas reached the highest number of cumulative deaths at (44%) as represented in **Figure *2.1.2*** [17].

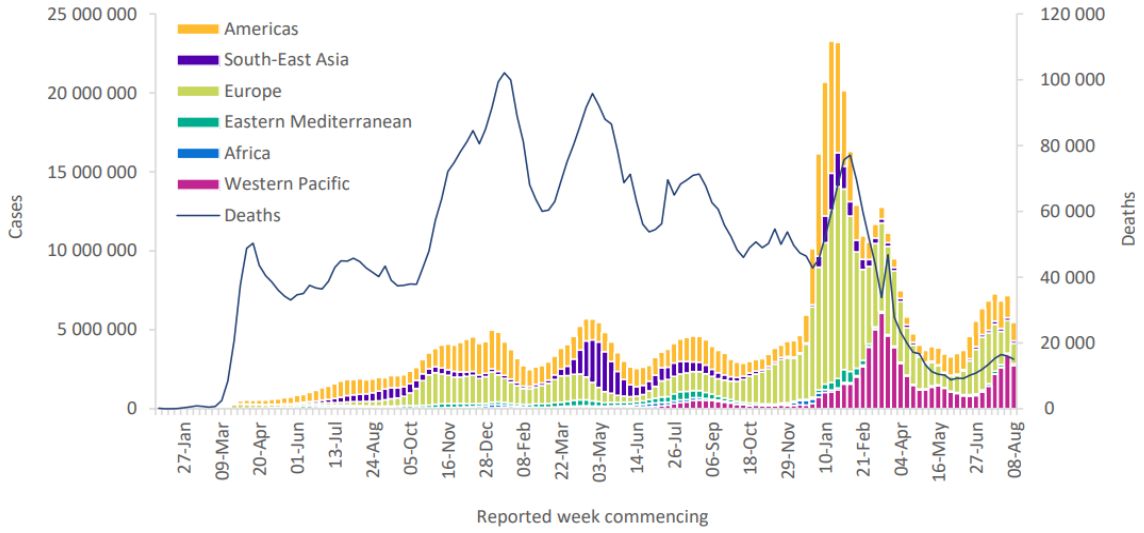

Figure 2.1.2 Weakly COVID-19 report of global cases and deaths as of August 14, 2022 (adapted from [17])

2.2 Virology of SARS-CoV-2 and Life Cycle

The single-stranded RNA virus, SARS-CoV-2, has similarities to the previously studied MERS-CoV and SARS-CoV viruses, which were responsible for the 2003 Severe Acute Respiratory Syndrome (SARS-CoV) pandemic and the 2012 Middle East Respiratory Syndrome (MERS) pandemic [18]. It's composed of four main structural proteins: envelope glycoprotein (E), spike (S), nucleocapsid (N), and membrane protein (M) [19] which can be observed in **Figure 2.2.1**.

Its envelope spike protein can recognize the entry receptor found in humans, angiotensin-converting enzyme II (ACE2), and once connected, plasma membrane fusion occurs. Plasma membrane fusion consists of the host's transmembrane serine protease 2 protein (TMPRSS2) performing the cleavage of the viral's spike protein, enabling the connection between the virus and the host's cell. Once fully connected, the virus enters the host's, cell infecting it [20].

Once inside, the virus can rapidly replicate itself, spreading within the human organism. ACE2 receptors are extremely common in a variety of human organs, being found in the enterocytes of the digestive system, myocardial cells, bladder urothelial cells, and others, thus leading to symptomatology related to these organs in COVID-19 patients, and multiple organ failure in critical patients [21,22].

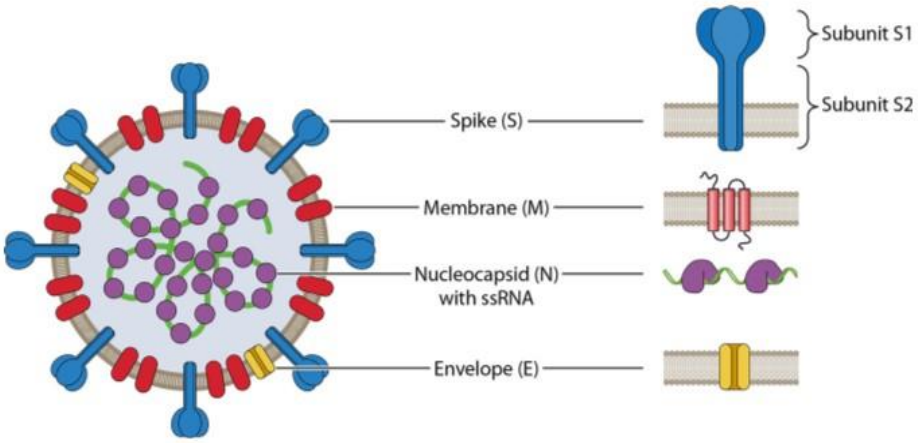

Figure 2.2.1 SARS-CoV-2's structure and main components (Adapted from [19])

2.3 COVID infection in the critical patient

COVID-19 is associated with mild to moderate symptoms in most of the population. Infections tend to lead to persistent coughing, fever, muscle aches and other similar symptoms to the common cold [23]. Even so, a smaller percentage of individuals are at risk of severe infection, often requiring hospital admission, suffering from long-term COVID-19 or even death [24]. As age advances, the incidence of various comorbidities increases significantly. Individuals with multiple comorbidities tend to present weaker immune systems and a higher predisposition for more severe complications [25,26].

Critical patients are associated with a hyperinflammatory state that leads to ARDS. Once ARDS sets in, several more complications are likely to onset, such as cardiac failure and multiple organ dysfunction syndrome [27]. Causes for ICU admission can include hypoxemic respiratory failure, ARDS, cardiac dysfunction, hepatic and/or renal dysfunction, among others [28]. Common comorbidities like diabetes, cardiovascular disease, lung and liver disease, chronic kidney disease, and obesity can severely worsen survival chances [25].

The innate immune system's role is to restrict viral replication within infected cells, as well as signaling the cells capable of defending the system, and setting up the adaptive immune system, allowing for a more efficient defense against reinfection [29].

Previous studies mention the importance in Type I interferon in the innate immune response against the SARS-CoV-19 virus [30,31]. The expression of this interferon, results in the efficient defense against viral replication. More severe forms of infection tend to show dysregulation of Interferon production, decreasing severely as patients become critical.

Lower levels of Type I Interferon lead to higher viral loads in peripheral blood, as well as an onset of severe pathological responses and inflammation leading to the complications previously mentioned such as ARDS, and organ failure [29]. The SARS-CoV-2 virus has shown to be able to efficiently develop strategies to antagonize IFN responses. If the virus is able to evade immune system defenses, it may lead to delayed IFN-I signaling, giving enough time for the virus to replicate, which combined with a hyperinflammatory response will cause damage to the lungs leading to ARDS. [29,30,32].

Critical cases tend to require some form of ventilation, as well as others invasive technique like central venous catheters (CVC) to sustain a steady recovery. Some treatments during the COVID-19 have patients undergo mechanical invasive ventilation, as well as in some cases, extra-corporeal membrane oxygenation (ECMO), which as of now, has insufficient studies correlating its use to better outcomes for severely ill COVID-19 patients. Due to the lack of a positive correlation between ECMO treatment and improvement of COVID-19 it isn't advised for effective treatment. Its use has also been confirmed to be a major risk for ICU-acquired bacteremia [33].

2.4 Bacteremia in the critical patient

Bacteremia is described as the presence of bacteria in the bloodstream [34]. It's recognized to be a heavy predecessor for morbidity and death worldwide [35]. Even with improvement of antimicrobial treatments and means of diagnosis, infection in the bloodstream is still extremely difficult to treat due to the urgency associated with correct treatment.

Involving the identification of the specific bacteria, and its characteristics, such as antibiotic sensitivity, is required for determination of correct antibiotic therapy for effective elimination of the pathogen. The complete process, which includes sampling, culture growth and gram-stain testing is extremely time consuming and may require days for completion. In a past study, blood culture has a sensitivity of 0.25 and an Area under curve (AUC) of 0.63 [36]. In the case of bacteremia, the prognostic worsens severely as time passes, allowing for infection to spread and initiate sepsis. Sepsis is characterized the presence of multiplying bacteria in the blood system, leading to a dysregulated host 'response to infection, causing organ dysfunction, which can become permanent and lead to death [37–39].

Common procedures in hospital settings may present themselves as gateways for bacterial infection. Patients with longer hospital stays, and especially ICU, are more susceptible to nosocomial infections [40,41]. Nosocomial infections are defined as a hospital acquired infection that develops within 48 to 72 hours after admission. ICU are inherently at a higher risk of nosocomial infection. Previous studies showed ICU patients represent a higher infection rate, with cases reporting up to 51% of all admitted [5].

These infections may be classified central line-associated bloodstream infections (CLABSIs) as central venous catheter bloodstream infections (CVCBSI), catheter-associated urinary tract infections (CAUTI), and ventilator-associated pneumonia (VAP) [42,43] .

Post-surgery patients and burn victims also tend to be easy targets for infection due to recent wounds susceptible for bacteria entry [44]. If infection occurs, time of hospitalization stay tends to increase, as treatment expenses get higher and survival rate decreases [45,46].

The ICU has become the center of infection, as well as the catalyst for antibiotic resistant bacteria growth. Critical patients tend to be receptors for an exacerbated amount of broad-spectrum antibiotics, to treat an unspecified infection while correct bacterial identification takes place [4,47]. This has severe consequences, as it results in rapid mutations, which can increase antibiotic resistance, leading to prolonged hospital stays, costs of treatment and higher mortality rates [48].

As antibiotic resistant bacteria grow and spread within the community, critical patients are extremely at risk of infection and sepsis, complicating treatment and leading to higher mortality.

Antibiotic resistance is a growing worldwide issue, that can prove to be fatal for many future patients, as bacteria become accustomed to various antibiotics, becoming stronger, and being able to defend themselves from general treatment. Not only that but as most antibiotics become weak for newly mutated bacteria, the prices for newer and improved treatment forms will skyrocket, reducing availability for a significant number of people. Medical procedures, like transplants and surgeries, even of lower risk, will be significantly riskier as infection gets harder to prevent and treat [49,50].

Bacteremia may be caused by Gram-Positive or Gram-Negative bacteria.

The identification of the bacteria causing infection is extremely important, and so is identification of its Gram-Stain. Knowing what type of Gram-Stain the bacteria possess allows for efficient selection of antibiotic for treatment, therefore reducing the exacerbated spread of multidrug-resistant pathogens [51].

The main reason for the discrepancy in antibiotic susceptibility between Gram-positive and Gram-Negative bacteria is the different structures of their cell wall **Figure 2.4.1**

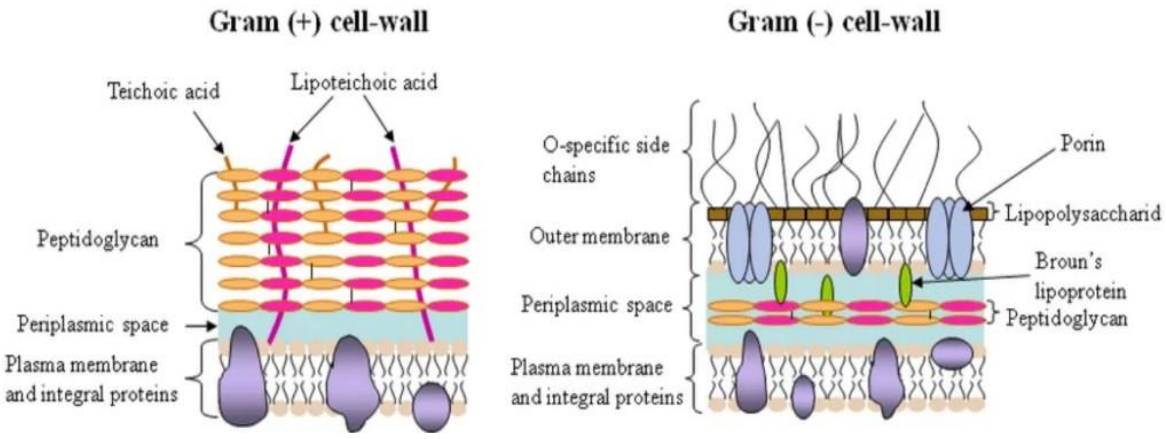

Figure 2.4.1 Gram-Positive and Gram-Negative cell wall structure

The composition of Gram-Negative's cell wall includes a lipopolysaccharide layer (PLS), while the Gram-Positive doesn't. This leads to a higher resistance to anti-microbials since the cell is more protected. Therefore, Gram-Negative bacteria tend to be associated with severe sepsis, and higher infection rates in the ICU [52].

Some of the most common forms of Gram-Positive and Gram-Negative bacteria associated with bloodstream infections can be found in **Table 2.4.1** [53,54]:

Table 2.4.1 Most common Gram-Positive and Gram-Negative bacteria associated with bacteremia.

Gram-Positive	Gram-Negative
Staphylococci aureus	*Escherichia coli*
Enterococcus faecalis	*Pseudomonas aeruginosa*
Streptococcus agalactiae	*Klebsiella pneumoniae*

In the events of inflammation and infection, certain metabolites may display behavioral changes, like increasing or reducing production concentrations to improve healing. The most reported ones are C-reactive protein (CRP, Procalcitonin (PCT), Interleukin-6 (IL-6) and Cluster of differentiation 64 (CD64).

2.5 Infection Biomarkers of interest

2.5.1 C-Reactive Protein

C-Reactive Protein is a biomarker heavily associated with inflammatory phenomena, rising its baseline concentration of 0,8 mg/L by a thousand times in acute inflammatory processes [55–57].

Originated as one of the pentraxins family, CRP is produced in the liver in the form of native C-reactive, composed by 5 monomers that dissociate irreversibly once inflammation or infection initiates. CRP is characterized by having a short half-life of 19 hours. Previous studies pinpointed the relevance of CRP as a biomarker for infection. It's released passively, whilst showing increased release in the presence of inflammatory cytokines such as interleukin 6 (IL-6) [58–62]. Other performed studies tried to determine diagnostic accuracy of CRP, by analyzing its specificity and sensitivity to diagnose bacteremia, and found that, for example, in the case of study [63]; CRP showed a limited capacity for bacteremia diagnosis, just merely reaching a top AUC 0.62 (95% CL, 0.57-0.67) on the first of three days analyzed in n=175 ICU patients admission [61,62].

2.5.1 Interleukin-6 (IL-6)

Interleukin-6 is a potent proinflammatory cytokine which is released by immune cells in the event of inflammation or infection [64]. It's secreted by a large array of cells and regulates the acute-phase response. Under certain circumstances, it may act as an anti-inflammatory cytokine [65]. It has been determined to have a significant role in the transition from neutrophiles to monocyte recruitment in the acute-phase response. It also plays a key role in the transition from acute-phase response to chronic inflammation [66].

Once IL-6 is synthetized, its transported into the liver by the bloodstream, where it'll induce the production of anti-inflammatory molecules like the CRP [57,60,64].

A meta-analysis was previously conducted involving 6 studies that analyzed the potential of IL-6 in diagnosing bacteremia in cirrhotic patients. The results showed an overall good sensitivity and specificity of 0.85 (95% CI, 0.64–0.94), 0.91 (95% CI, 0.80–0.96), respectively. Nonetheless, the studies included all had distinct cut-off values for IL-6's serum concentrations, leading to inconclusive results, therefore requiring further investigation [67].

2.5.2 Procalcitonin

Procalcitonin (PCT) is a precursor protein of the calcitonin hormone. The codifying gene (CALC-1), in standard conditions, is exclusively expressed in parafollicular cells. Parafollicular cells, or C cells, are neuroendocrine cells found in the thyroid. As the CALC-1 gene is activated, produced PCT is stored in the Golgi complex. In the occurrence of systemic infections, the gene is positively regulated, leading to mass PCT production, thus drastically increasing its bloodstream concentration. PCT has a superior half-life to CRP, approximately between 22 to 29 hours.

Previous studies determined that in case of bacterial infection, concentration reaches a production peak between 12 to 14 hours after initiation of the infection [61,68,69]. A meta-analysis intended to compile and determine the overall AUC, complete with pooled sensitivity and specificity of 58 studies on using procalcitonin for bacteremia identification in ICU patients. The overall AUC corresponded to 0.88 with a pooled specificity of 68 (95%, 0.57-0.77) and a sensitivity of 89 (95%, 0.79-0.94). As in the case of CRP, procalcitonin also shows high sensitivity, although showing a low specificity for bacteremia, decreasing its potential as an accurate biomarker [70].

2.5.3 Cluster of differentiation 64 (CD64)

The CD64 neutrophile is mostly found on the surface of macrophages, dendritic cells, and monocytes. Whilst baseline values are low, in the event of infection its concentration rapidly increases and consequently, the immune system is activated. It invokes the massive release of polymorphonuclear neutrophils (PMN), such as neutrophiles, eosinophils and basophils, that act on the phagocytose and destruction of the pathogen. Previous studies aimed to show how effective the CD64 neutrophile is as a biomarker for infection and sepsis in critical patients, ranging from post-operative to hematological malignancies [71–73].

CD64 has been studied for its accuracy in bacteremia diagnosis for years, and even has been considered by some studies to be more effective than using CRP or PCT in some cases. In a meta-analysis comprising the accuracies of 11 studies, CD64 showed a pooled AUC of 0.89 (95% CI, 0.85-0.94), a sensitivity of 0.89 (95% CI, 0.83–0.94) and a specificity of 0.91 (95% CI, 0.87–0.95), which proves the potential of CD64 as a bacteremia biomarker in critical patients [74].

2.5.4 Biomarker accuracy

These biomarkers are known to be associated with aggravated COVID-19 and additionally, in the event of acute inflammatory response, all of these tend to increase production. Since ICU patients tend to suffer from extreme inflammatory processes during their recovery or treatment, it becomes extremely difficult to rely on any of these as full-proof bacteremia biomarkers [27,75–77]. Therefore, a study that aims to determine a new biomarker, with better specificity and sensitivity towards bacteremia, is extremely important and of elevated interest, to improve not only critical patients with severe COVID-19, but also every single patient admitted to the ICU, since a quicker and more efficient diagnosis will improve upon earlier and accurate diagnosis, which reduces morbidity and mortality [78–80].

2.6 Fourier-transform Infrared spectroscopy

This thesis approaches bacteria and gram strain identification by using Fourier-transform Infrared Spectroscopy (FTIR). FTIR is an infrared (IR) spectroscopy method that allows for accurate determination of functional groups, bonding types, and molecular conformations within a sample (gas, liquid or solid), by measuring the amount of radiation that molecules absorb from a striking IR beam at specific wavelengths, causing molecular vibration. Once the sample is analyzed, a “fingerprint” for each of the compounds is identifiable, allowing for full biochemical characterization of the sample.

FTIR spectroscopy has been increasingly used in studies that need to identify biological sample's functional composition, in order to aid diagnosis of several diseases, such as cancers [81,82].

Infrared radiation is a section of the electromagnetic spectrum, composed of three main regions: near-IR (NIR), mid-IR (MIR) and far-IR (FIR) [83].

In this study, the region of interest is the MIR, due to it being the most appropriate region for study of fundamental vibrations and structural composition of the sample's molecules [84]. Previous studies utilized MIR to its full potential and provided insight into how its use can be useful in identification of various compounds, ranging from proteins [85], to nucleic acids [86]. The FTIR spectroscopy process begins by emitting an IR beam, which originates from a black body source, into an interferometer.

The interferometer is a measurement method that consists of splitting a beam into two separate beams, one that strikes a fixed mirror, and another one striking a movable mirror. These are then reflected, causing superposition, and creating an interference pattern. If the phase difference is equal to zero, the beams will interfere constructively, thus creating a high intensity signal. This allows for the acquisition the spectral information of all wavelengths. Once the beam is recomposed, it passes through the sample and into the detector [87,88]. A visual representation can be observed in **Figure 2.6.1**.

The detector will then create a raw data analysis comparing light intensity and mirror position, which then Fourier-transforming processes for a single channel reference spectrum. Simultaneously a beam is superimposed to create a reference for instrumentation operation. In the end, the IR spectrum from FTIR spectroscopy is acquired by subtracting the reference spectrum from the spectrum provided by the sample analysis [87,89].

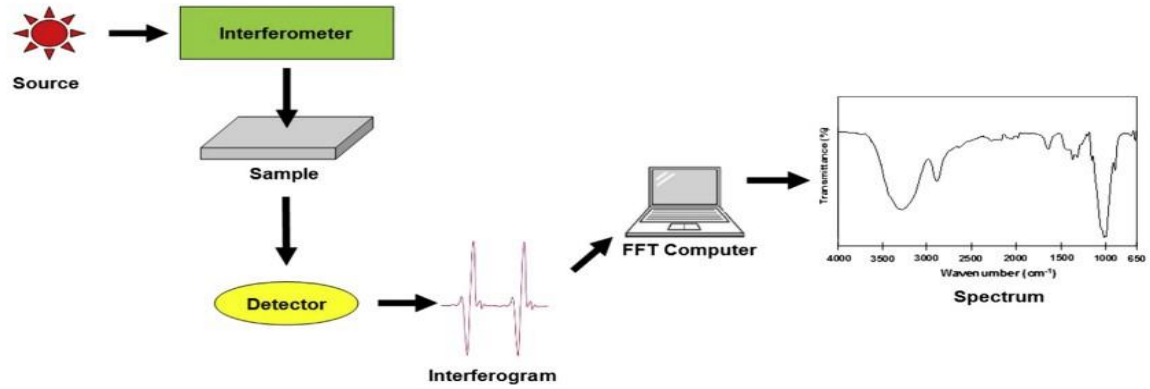

Figure 2.6.1 Basic components in FTIR

The FTIR spectroscopy spectrum can be divided into two main sections: the Functional Group Region (FGR), and the Fingerprint region as shown in **Figure 2.6.2** [90,91]. The functional group region allows for examination of functional groups within the sample, which can be compared to spectrum from pure compounds to correctly identify the different compounds in the sample. The Fingerprint region allows for precise analysis, since characteristics as small as structural differences and molecule composition, may result in significant variation of the distribution of the absorption bands corresponding to this region. Therefore, compounds tend to display almost identical fingerprint regions, which are easily recognizable [92].

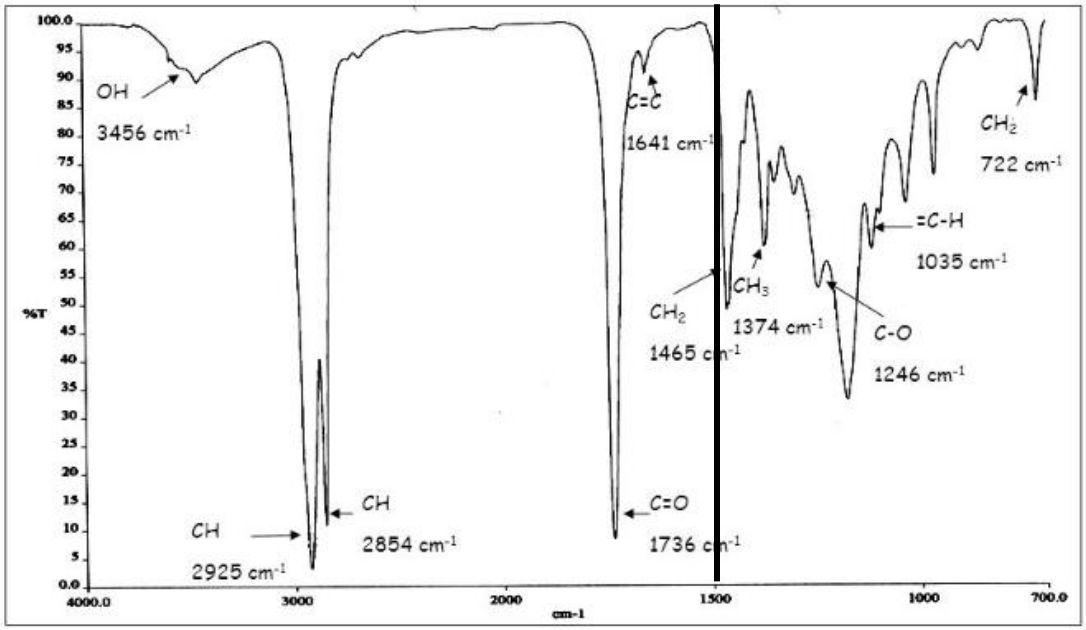

Functional Group Region **Fingerprint Region**

Figure 2.6.2 FTIR Specter with defined Functional Group and Fingerprint regions (adapted from [75])

The functional group of the FTIR spectroscopy spectrum includes the single bond, double bond, and triple bond areas. There are four regions that may be analyzed in the FTIR spectroscopy spectra, which are listed in **Table *2.6.1***.

Table 2.6.1 Regions of the FTIR spectroscopy Spectra and corresponding wavelengths

Region	Wavelengths
Single Bond	2500-4000 cm^{-1}
Double Bond	1500-2000 cm^{-1}
Triple Bond	2000-2500 cm^{-1}
Fingerprint	650-1500 cm^{-1}

Along the years, FTIR spectroscopy has become a staple methodology for a multitude of clinical studies, such as infection typing [93–95] and bacterial typing [96–98]. It has proven to be effective and an easy, low-cost, and fast methodology, justifying its use in this thesis for infection and bacteria related analysis.

3 Methodology

3.1 Study population and demographic data

Patients that entered the targeted sample were originally members of a group of hospitalized individuals, that required intensive care in the ICU of *Hospital Universitário Lisboa Central*, between the months of November 2020 and September 2021. These patients were admitted for a multitude of reasons, with Acute respiratory failure – COVID 19 being the most persistent (90,2%). These were all tested for COVID-19, by reverse-transcriptase-polymerase-chain-reaction-reaction (RT-PCR) assay. The present study is inserted in the Predictive Models of COVID-19 Outcomes for Higher Risk Patients Towards a Precision Medicine (PREMO), approved by the previously mentioned board of ethics and under all legal and ethics considerations.

Data from the raw sample was condensed in a data base in the platform Microsoft Excel. This database consists of demographical data like: RT-PCR diagnosis, dates from hospital/ICU admission and discharge; comorbidities and reasons for admission, as well as other relevant information. All the information was gathered from the hospital electronic medical record system. Various other tests that were also performed to each patient, was also acquired, in singular Microsoft Excel files. The tests performed included hemograms, urine tests, blood gas analysis, as well as daily metabolite measurements.

The starting sample was composed of 512 patients. Patients under 18 years of age and without enough relevant information for study composition were excluded (n=1). Patients without hospital/ICU date of admission; a negative RT-PCR test were also removed from the sample (n=198). From the remaining 313 patients, were selected patient' with serum samples in the present laboratory presenting bacteremia, i.e., presenting bacterial infection in the blood, for a targeted group (n=48) and a control group, composed of patient samples clear of bacteremia (n=54).

3.2 Clinical and Demographic Data

The sample was organized by age, gender, body mass index (BMI), presence, and number of comorbidities. Data such as age and patient's gender were calculated from obtained data at admission. The patients were divided into the following age groupings: 30 years or younger; 30 through 39 years; 40 through 49 years; 50 through 59 years; 60 through 69 years; 70 through 79 years and 80 years or older.

BMI was calculated by dividing the weight in kilograms by the meters squared. Since height was measured in centimeters, the result was multiplied by 10000. BMI was the main way to measure obesity degrees. The BMI categories are classified as less or equal to 29,9 Kg/m2 (normal BMI); 30 through 34,9 Kg/m2 (Class I Obesity); 35 through 39,9 Kg/m2 (Class II Obesity); and equal to or greater than 40 Kg/m2 (Class III Obesity) [99].

Comorbidities among patients were accounted for, and patients were grouped by number of comorbidities. The comorbidities groupings were as follows: 0 comorbidities; 1 to 2 comorbidities; 3 to 4 comorbidities; 5 or more comorbidities.

Patients who required respiratory support like IMV and ECMO, were identified, as well as the duration of the respective treatment.

3.3 Statistical analysis

All relevant variables were analyzed regarding its typology and the data type. Categorical variables such as comorbidities and gender, were presented by their absolute frequencies and percentages, whilst categorical variables were represented with medians and interquartile range (25^{th} percentile-75^{th} percentile). This presentation is justified by the fact the results regarding these variables, follow an asymmetric distribution and deviates from statistical normality. To obtain p values for each of the compared variables, either the χ^2 for qualitative variables or the T-test for quantitative variables. Each test, if the P values equivalent to ≤0.05, it's assumed that the variables are statistically different. Tests are identifiable in **Table 4.1.1** and **Table 4.1.2**. by the symbol code presented in **Table 3.3.1**.

Chi squared were determined in the IBM® SPSS® Statistics version 26 software while T-testing occurred in the Microsoft Excel software from Microsoft Corporation.

Table 3.3.1 Tests and attached symbols for interpretation.

Test	Symbol
Chi-squared	×
T-Test	▪

3.4 Spectral data acquisition and spectra data processing

In this study, the FTIR spectra was obtained by serum analysis. Serum has been widely used for metabolomic studies, since it has shown to have higher metabolite concentrations, making it easier for detection and quantification [100]. Other studies that utilized the potential of serum to pursue biomarker detection can be read by following the bibliography through [101,102]. The serum samples used in this study were prepared by Dr. Rubén Araujo, by firstly collecting a sample of 3 mL of patient's blood with EDTA from patients admitted to the CHULC's ICU. From that, then preceded the plasma extraction and, as such, the serum. This process took less than 12 hours. The obtained serum was then processed and stored in duplicates, at -20 ºC.

3.5 Data processing and analysis

Pre-processing of FTIR spectrum allows for the removal of physical phenomena or noise that may interfere with exploratory analyses. The following pre-processes methods were analyzed:

- atmospheric correction and baseline;
- atmospheric correction, baseline, and Unit Vector Normalization (UVN);
- atmospheric correction followed by 2nd Derivative (2nd Degree polynomial with 15 points);
- atmospheric correction followed by 2nd Derivative (2nd Degree polynomial with 15 points) and UVN;
- 2nd Derivative (2nd Degree polynomial with 15 points) within the ranges of 600-1800 cm^{-1} and 2800-3100 cm^{-1};
- 2nd Derivative (2nd Degree polynomial with 15 points) and UVN within the ranges of 600-1800 cm^{-1} and 2800-3100 cm^{-1};

The individual objective of each preprocessing can be found in **Table 3.5.1**.

Table 3.5.1 Preprocessing with corresponding goal.

Pre-Processing	Goal
Atmospheric correction	Removal of the effects of the atmosphere
Baseline	Used to adjust the spectral offset by adjusting the data do the minimum point in the data
Unit Vector Normalization	Used to equally scale samples
2nd Derivative (2nd Degree polynomial with 15 points)	Used to smooth out data
Selection of wavelength ranges (600-1800 cm^{-1} and 2800-3100 cm^{-1})	Focusing analyses on the ranges of interest

The impact of each pre-processing method was evaluated on non-supervised principal component analysis (PCA) and hierarchical cluster analysis (HCA), which allow for the clustering of similar groups, with adequate visual representation.

PCAs used the non-linear iterative partial least squares (NIPALS) algorithm, whilst the algorithm used for “Gram-positive versus Gram-negative” analyses was Singular Value Decomposition (SVD) model input, both with a maximum of 7 components. The different selection of algorithm was automatically selected by the program used, with Scramble. NIPALS enables the analysis when there are missing values, whilst SVD can’t. All wavenumbers had equal weight and were cross validated randomly with 20 segments (5 samples each). Hotelling curve was selected at 1%, i.e., 99% variance.

HCA analyses was performed by selecting a preference of 2 clusters, one corresponding to each targeted group, and by combining a selection of clustering methods with distance measure correlations. The clustering methods were Hierarchical Single linkage, Hierarchical Complete linkage, Hierarchical Average linkage and Hierarchical Median linkage and Ward’s method. Further detailing on the functions of each can be found in **Table 3.5.2**. All of these were combined with Spearman’s rank correlation and Euclidian for distance measurement, individually, to test multiple variations and obtain the best result possible.

Table 3.5.2 List of linkage methods and corresponding grouping criteria.

Linkage Methods	Function
Single linkage	Grouping by closest distance between samples
Average linkage	Grouping by average distance between samples
Median linkage	Grouping by the geometrical distance between samples
Complete linkage	Grouping by the farthest distance between any two samples for its basis
Ward's method	Aims to maximize the homogeneity of the groups

The supervised linear discriminant analysis (PCA-LDA) method was performed, varying the number of components from 2 to 7. PCA-LDA is used to reduce the number of features of a sample, to obtain a more manageable set of data. The result is a linear function that represents the difference between two groups. The difference between the groups, or the separation, improves as the variance between groups increases and the variance within the groups decreases. The test consists of composing a calibration and a validation group within the sample. The calibration group was composed of two thirds of the sample, while the remaining one third was used to test the classification efficiency.

All the evaluation process was conducted in The Unscrambler X™ program version 10.4. and all of the information gathered about the analyses were gathered in its user manual [103].

4 Results and discussion

This chapter is divided into two main sections. In the first section, the goal was to evaluate the FTIR based discrimination between Bacteremia (n=48) and non-Bacteremia patients (n=54) through PCA, HCA and LDA analyses.

The second section aimed to evaluate the FTIR based discrimination in patients with bacteremia, if were Gram-Positive (n=28) or Gram-Negative (n=20) bacteria.

4.1 Clinical and demographic characteristics

Clinical characteristics and demographics of the patients included in this study are detailed in **Table 4.1.1**. The complete sample is composed of 102 patients with COVID-19, all admitted to the ICU. The sample's median age corresponded to 59 years old (P_{25}= 51; P_{75}=69), ranging between 19 to 88 years old. More than 70% of the patients have more than 50 years old, as expected, as age is a critical factor for COVID-19 severity. Only a residual percentage of 3.9% are below 30 years old.

The sample is composed for the most part by male patients, corresponding to 73.5% of the sample, with a total number of 75 patients. Weight and heights were measured to calculate corresponding BMI's. A total of 10 patients had no determinable BMI value due to missing height or weight values. Missing patients accounted for 5% (n=5). BMI median corresponded to 27,7 (P_{25}= 24,7; P_{75}=31,1) Kg/m^2. Most patients had a calculated BMI of lesser or equal to 29,9 Kg/m^2 (70.7%), indicating that 29.3% are at least obese.

Most patients had at least one comorbidity (85.3%), with Arterial Hypertension (50%), Diabetes mellitus (32.4%), obesity (30.4%) and dyslipidemia (37.5%) being the most common comorbidities. Other comorbidities were residuals in comparison, with only alcoholism and smoking habits standing out at 10.8% and 15.7%, respectively. Admission motives were particularly one-sided with a majority being admitted for medical causes (95.1%) associated with COVID-19 induced ARDS (90.2%). Invasive mechanical ventilation (IMV) and ECMO were applied in 85, and 20 patients respectively. The median of IMV days was 14 days (P_{25}= 8.3; P_{75}=40.3) and of ECMO of 10 days (P_{25}=5; P_{75}=18). ICU stay had a median of 10 days (P_{25}= 2; P_{75}=102).

Table 4.1.1 Demographic data from all patients and comparisons between patients with bacteremia and patients without bacteremia. T-tests are represented by ▪, and Chi-Squared tests are represented by ×.

Variables N (%)	Total Missing's n (%) / N	All Patients (n=102)	Bacteremia Patients (n=48)	Patients without Bacteremia (n=54)	P
Gender					
Female	-	27 (26.5)	11 (22.9)	16 (29.6)	0.443 ×
Male	-	75 (73.5)	37 (77.1)	38 (70.4)	
Age					
Age (years)	-	59.5 (50.8-69.3)	58 (51.3-66)	54 (47-71.3)	0.507 ▪
Age groups					
<30 years	-	4 (3.9)	2 (4.2)	2 (3.7)	0.093 ×
30-39 years	-	11 (10.8)	4 (8.3)	7 (13)	
40-49 years	-	8 (7.8)	2 (4.2)	6 (11.1)	
50-59 years	-	28 (27.5)	18 (37.5)	10 (18.5)	
60-69 years	-	26 (25.5)	13 (27.1)	13 (24.1)	
70-79 years	-	19 (18.6)	9 (18.8)	10 (31.3)	
≥80 years	-	6 (5.9)	0 (0)	6 (19)	
Peso (Kg)	5 (5%)/102	80 (75-90)	80 (75-90)	80 (70-90)	0.184 ▪
Altura (Cm)	10 (10%)/102	170 (150-190)	170 (150-190)	170 (150-185)	0.249 ▪
BMI					
BMI. Kg/m^2	10 (9.8%) /102	27.7 (24.7-31.1)	27.6 (24.7-32)	27.7 (24.6-29.8)	0.401 ▪
BMI Categories					
≤29.9 Kg/m^2	10 (9.8%)/102	65 (70.7)	30 (65.2)	35 (76.1)	0.644 ×
30-34.9 Kg/m^2		14 (15.2)	9 (19.6	5 (10.9)	
35-39.9 Kg/m^2		6 (6.5)	3 (6.5)	3 (6.5)	
≥40 Kg/m		7 (7.6)	4 (8.7)	3 (6.5)	
Presence of Comorbidities					
Yes	-	87 (85.3)	44 (91.7)	43 (79.6)	0.086 ×
No	-	15 (14.7)	4 (8.3)	11 (20.4)	
Comorbidities					
Arterial Hypertension	-	51 (50)	23 (49.9)	28 (51.9)	
Diabetes mellitus	-	33 (32.4)	15 (31.3)	18 (33.3)	
Dyslipidemia	-	23 (22.5)	18 (37.5)	6 (11.1)	
Obesity	-	31 (30.4)	18 (37.5)	14 (25.9)	
Asthma	-	5 (4.9)	3 (6.3)	2 (3.7)	
COPD	-	6 (5.9)	41 (85.4)	19 (35.2)	
Alcoholism	-	11 (10.8)	7 (14.6)	4 (7.4)	
Extrinsic Allergic Alveolitis	-	1 (1)	0	1 (1.9)	
Andropause	-	1 (1)	0	1 (1.9)	
Iron Deficiency Anemia	-	1 (1)	0	1 (1.9)	
Descending thoracic aortic aneurysm	-	1 (1)	1 (2.1)	0	
Angina	-	1 (1)	0	1 (1.9)	
Smoker	-	16 (15.7)	12 (25)	4 (7.4)	
Stroke	-	4 (3.9)	1 (2.1)	3 (5.6)	
Congenic Cardiopathic	-	1 (1)	0	1 (1.9)	
Ischemic Heart Disease	-	1 (1)	1 (2.1)	0	
Peripheral Arterial Disease	-	3 (2.9)	2 (4.2)	1 (1.9)	
Depression	-	4 (3.9)	4 (8.3)	0	
Chronic Liver Disease	-	1 (1)	1 (2.1)	0	
Chronic Kidney Disease	-	4 (3.9)	2 (4.2)	2 (3.7)	
Acute Myocardial Infarction	-	1 (1)	0	1 (1.9)	

HIV Positive	-	2 (2)	2 (4.2)	0	
History of Organ Transplantation	-	3 (2.9)	1 (2)	1 (1.9)	
Hypothyroidism	-	5 (4.9)	1 (2.1)	4 (7.4)	
Neo	-	5 (4.9)	2 (4.2)	3 (5.6)	
Obstructive Sleep Apnea Syndrome	-	6 (5.89)	3 (6.3)	3 (5.6)	
Renal Insufficiency	-	4 (3.9)	2 (4.2)	2 (3.7)	
Number of Comorbidities					
0 comorbidities	-	15 (14.7)	4 (8.3)	11 (20.4)	
1-2 comorbidities	-	33 (32.4)	17 (35.4)	16 (29.6)	0.386 ×
3-4 comorbidities	-	33 (32.4)	17 (35.4)	16 (29.6)	
≥5 comorbidities	-	21 (20.6)	10 (20.8)	11 (20.4)	
Types of Patients at Admission					
Medical	-	97 (95.1)	47 (97.9)	50 (92.6)	
Surgical (Urgency) and Trauma	-	3 (2.9)	1 (2.1)	2 (3.7)	
Medical - coronary	-	1 (1)	0	1 (1.9)	
Trauma (With neurotrauma)	-	1 (1)	0	1 (1.9)	
Admission Motive					
Acute Respiratory Failure (ARDS)	-	2 (2)	1 (2.1)	1 (1.9)	
COVID-19 induced ARDS	-	92 (90.2)	45 (93.8)	47 (87)	
Septic Shock or Sepsis	-	1	1 (2.1)	0	
Cardiac Arrest	-	2 (2)	0	2 (3.7)	
ARDS/ALI	-	2 (2)	1 (2.1)	1 (1.9)	
Coma	-	1 (1)	0	1 (1.9)	
Monitoring	-	2 (2)	0	2 (3.7)	
Respiratory Support					
IMV	-	85 (83.3)	46 (95.8)	39 (72.2)	0.001 ×
ECMO	-	20 (19.6)	15 (31.3)	5 (9.3)	0.006 ×
Treatment duration (Days)					
ICU	-	10 (2-102)	18 (9.1-25.2)	6 (3.9-11.1)	<0.001 ▪
ECMO	-	14 (8.3-40.3)	31 (10-46)	9 (3.5-11.5)	0.058 ▪
IMV	-	10 (5-18)	15 (8-28)	6 (4-11)	<0.001 ▪

P-values for studied variables were obtained with a significance level of 5%

To group and compare clinical and demographical data for the second comparison group, “Gram-Positive versus Gram-Negative” an additional table was created. There’s a total of 48 patients, 28 with Gram-Positive bacteremia and 20 with Gram-Negative bacteria. Patients tend to similarly show a higher male percentage, with 78.6% and 75% of patients presenting Gram-Positive and Gram-Negative bacteria being males. Age median is similar between target groups with age values of 60 and 56 years old (Gram-Positive: P_{25} = 51; P_{75} = 68.5; Gram-Negative: P_{25} = 52.5 P_{75} = 61.8), for Gram-Positive and Gram-Negative bacteria groups, respectively. Clinical data like weight, height, BMI, all resemble the data acquired for the previous targeted groups.

The variables “IMV”, “ECMO”, as well as “ICU treatment days” and “IMV days” were determined to be statistically significant, with a p value inferior to 0.05. This means the variables have a strong relation between bacteremia and non-bacteremia patients.

The complete sample for the second targeted analyses is composed of 48 patients with COVID-19 and bacteremia, all admitted to the ICU. The sample’s median age corresponded to 58 (P_{25}= 51.3; P_{75}=66), whereas the ages ranged from 26 to 79 years of age. Patients with Gram-Positive bacteria had a median age of 60 years (P_{25}= 51; P_{75}=68.5), while patients with Gram-Negative bacteria had a median age of 56.5 years (P_{25}= 52.5; P_{75}=61.8). Most patients in both groups (>50%) are of at least 50 years old. Only 12.5% of patients are younger than 40 years old. Weight and heights were measured to calculate corresponding BMI’s.

A total of 2 patients had no determinable BMI value due to missing height or weight values. Missing patients accounted for 4.2% (n=2). BMI median of the Gram-Positive group corresponded to 27,7 (P_{25}= 24,6; P_{75}=31,9) Kg/m^2 and Gram-negative’s median BMI corresponded to 27,5 (P_{25}= 25.2; P_{75}=34) Kg/m^2. Most patients had a calculated BMI of lesser or equal to 29,9 Kg/m^2 (65.2%), indicating that 34.8% are at least obese.

Most patients had at least one comorbidity (91.7%), with Arterial Hypertension (47.9%), Diabetes mellitus (31.3%), obesity (37.5%) and dyslipidemia (37.5%) being the most common comorbidities. The most common comorbidities among Gram-Positive bacteria patients were HTA and dyslipidemia, both being identified in a percentage of 53.6% of patients. In the Gram-Negative bacteria patient’s group, a higher percentage had present HTA and obesity, both with 40% of patients being previously diagnosed. Admission motives were 100% indicated as being for medical causes in the Gram-Positive group, whilst the Gram-Negative group was close to reaching the same percentage with only 1 patient (5%) being admitted for surgical (urgency) and trauma.

According to the global sample previously described, 92.9% and 95% of patients with Gram-positive or Gram-Negative bacteria blood infection, were admitted with COVID-19 with ARDS, respectively. All patients from the Gram-Negative group required IMV, whilst two patients from the Gram-Positive groups didn’t, therefore being used for 92.9% of patients. ECMO wasn’t as prevalent in either group as when comparing Bacteremia versus Non-Bacteremia, with only 9 patients from the Gram-Positive group and 6 from the Gram-Negative group requiring for the specific respiratory support. Finally, the Gram-Negative group had a higher median of days spent admitted to the ICU, with a median value of 22 days (P_{25}= 14.1; P_{75}=45.4). Data can be found in **Table *4.1.2***

Table 4.1.2 Clinical and demographical data for Gram-Positive versus Gram-Negative bacteria groups. T-tests are represented by ▪, and Chi-Squared tests are represented by ×.

Variables N (%)	Total Missing's n (%) / N	All Bacteremia Patients (n=48)	Gram-Positive (n=28)	Gram-Negative (n=20)	*P* value
Gender					
Female	-	37 (77)	6 (21.4)	5 (15)	0.772 ×
Male	-	11 (22.9)	22 (78.6)	15 (75)	
Age					
Age. years	-	58 (51.3-66)	60 (51-68.5)	56.5 (52.5-61.8)	0.501 ▪
Age groups					
<30 years	-	2 (4.2)	2 (7.1)	0	0.220 ×
30-39 years	-	4 (8.3)	1 (3.6)	3 (15)	
40-49 years	-	2 (4.2)	2 (7.1)	0	
50-59 years	-	18 (37.5)	8 (28.6)	10 (50)	
60-69 years	-	13 (27.1)	9 (32.1)	4 (20)	
70-79 years	-	9 (18.8)	6 (21.4)	3 (15)	
≥80 years	-	0	0	0	
Peso (Kg)	1 (2.1%) / 48	80 (75-90)	80 (75-90)	80 (76.3-90)	0.943 ▪
Altura (cm)	2 (4.2%) / 48	170 (150-190)	170 (170-180)	170 (170-180)	0.428 ▪
BMI					
BMI. Kg/m2	2 (4.2%) / 48	27.6 (24.7-32)	27.7 (24.6-31.9)	27.5 (25.2-34)	0.958 ▪
BMI Categories					
≤29.9 Kg/m2	2 (4.2%) / 48	30 (65.2)	17 (63)	13 (64.8)	0.921 ×
30-34.9 Kg/m2		9 (19.6)	6 (22)	3 (9.23)	
35-39.9 Kg/m2		3 (6.5)	2 (7.4)	1 (5.6)	
≥40 Kg/m		4 (8.7)	2 (7.4)	2 (5.6)	
Presence of Comorbidities					
Yes	-	44 (91.7)	27 (96.4)	17 (85)	0.158 ×
No	-	4 (8.3)	1 (3.6)	3 (15)	
Comorbidities	-				
Arterial Hypertension	-	23 (47.9)	15 (53.6)	8 (40)	
Diabetes mellitus	-	15 (31.3)	8 (28.6)	7 (35)	
Dyslipidemia	-	18 (37.5)	15 (53.6)	3 (15)	
Obesity	-	18 (37.5)	10 (35.7)	8 (40)	
Asthma	-	3 (6.3)	2 (7.1)	1 (5)	
COPD	-	4 (8.3)	3 (10.7)	1 (5)	
Alcoholism	-	1 (2.1)	1 (3.6)	0	
Iron Deficiency Anemia	-	1 (2.1)	1 (3.6)	0	
Descending thoracic aortic aneurysm	-	1 (2.1)	0	1 (5)	
Smoker	-	12 (25)	9 (32.1)	3 (15)	
Stroke	-	1 (2.1)	1 (3.6)	0	
Ischemic Heart Disease	-	2 (4.9)	0	2 (10)	
Depression	-	4 (8.3)	3 (10.7)	1 (5)	
Chronic Kidney Disease	-	2 (4.2)	1 (3.6)	1 (5)	
HIV Positive	-	2 (2)	2 (7.1)	0	
History of Organ Transplantation	-	1 (2.1)	0	1 (5)	
Hypothyroidism	-	5 (4.9)	1 (3.6)	4 (20)	
Neo	-	2 (4.2)	2 (7.1)	0	
Obstructive Sleep Apnea Syndrome	-	3 (6.3)	2 (7.1)	1 (5)	
Number of Comorbidities	-				
0 comorbidities	-	4 (8.3)	1 (3.6)	3 (15)	0.259 ×
1-2 comorbidities	-	17 (35.4)	9 (32.1)	9 (45)	
3-4 comorbidities	-	17 (35.4)	11 (39.3)	6 (30)	
≥5 comorbidities	-	10 (20.8)	7 (25)	2 (10)	

Type of Patients at Admission	-				
Medical	-	47 (97.9)	28 (100)	19 (95)	
Surgical (Urgency) and Trauma	-	1 (2.1)	0	1 (5)	
Admission Motive	-				
Acute Respiratory Failure (ARDS)	-	1 (2.1)	1 (3.6)	0	
COVID-19 induced ARDS	-	45 (93.8)	26 (92.9)	19 (95)	
Septic Shock or Sepsis	-	1 (2.1)	0	1 (5)	
ARDS/ALI	-	1 (2.1)	1 (2.1)	0	
Respiratory Support					
IMV		46 (95.8)	26 (92.9)	20 (100)	0.222 ×
ECMO		15 (31.3)	6 (21.4)	9 (45)	0.082 ×
Treatment duration (Days)					
ICU		18 (9.1-25.2)	13.5 (7.7-22.5)	22 (14.1-45.4)	0.155 ▪
ECMO		31 (10-46)	25 (12.3-46.5)	31 (6-44.5)	0.879 ▪
IMV		16 (8-28)	12 (6-20.5)	22 (9.3-35)	0.184 ▪

P-values for studied variables were obtained with a significance level of 5%

P-values weren't calculated if the variable's frequencies were too small/ null. P values weren't also calculated for the variables "Type of Patient at Admission" and "Admission Motive" because it wasn't clinically relevant.

Variables with less than 30 samples were assumed to not follow a normal distribution

In the case of gram-stain discrimination, the only variable to present statistically significant ($p \leq 0.05$) was "ECMO". Meaning there is a strong relation between use of ECMO on patients and the presence of Gram-Negative bacteria.

Identified bacteria and their respective frequencies among the Bacteremia patients can be found in **Table *4.1.3***.

Table 4.1.3 Identified Bacteria and frequency among patients with bacteremia included in sample

Bacteria	Frequency
Methicillin-resistant Staphylococcus aureus	2
Methicillin-resistant S.epidermidis	2
Enterobacter aerogenes	2
Enterobacter clocae	2
Enterococcus faecalis	2
Escherichia coli	3
Klebsiella oxytoca	2
Klebsiella pneumoniae	8
Pseudomonas aeruginosa	1
Methicillin-sensitive Staphylococcus aureus (MSSA)	11
Methicillin-resistant Staphylococcus epidermidis (MRSE)	2
Methicillin-sensitive Staphylococcus epidermidis (MSSE)	1
Serratia marcescens	2
Staphylococcus haemolyticus	1
Staphylococcus hominis	3
Staphylococcus lugdunensis	1
Streptococcus anginosus	1
Streptococcus gallolyticus	1
Streptococcus mitis/Streptococcus oralis	1

4.2 Bacteremia vs non-Bacteremia

Results for FTIR spectroscopy discrimination for Bacteremia versus non-Bacteremia patients in the global sample is presented by PCA, HCA and PCA-LDA analysis for each pre-processing described before in **Data processing and analysis.**

Both PCA and HCA results showed a lack of efficiency for separation between the two groups. Visual presentation of the best results obtained for both forms of analyses are presented in **Figure 4.2.1**, **Figure 4.2.2**, , **Figure 4.2.4**. The best PCA-LDA are presented in **Figure 4.2.5**

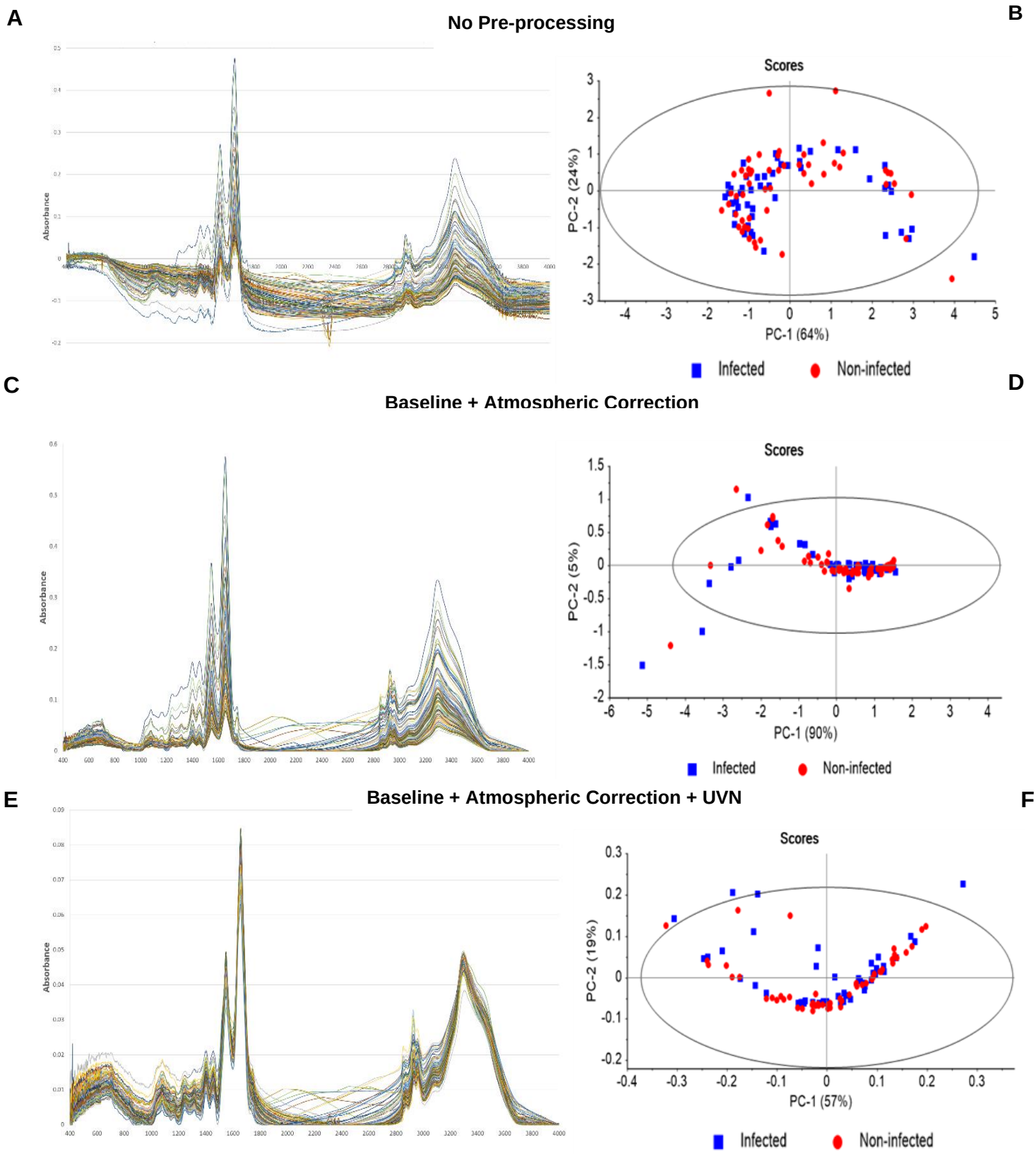

Figure 4.2.1 On the left side are spectra with different pre-processing methods, and on the right are the corresponding PCA between Infected with Bacteremia (Blue) and Not-Infected with Bacteremia (Red): (A&B) Without pre-processing; (C&D) Atmospheric and Baseline correction; (E&F) Atmospheric and Baseline with UVN.

2nd Derivative + Atmospheric correction

G

H

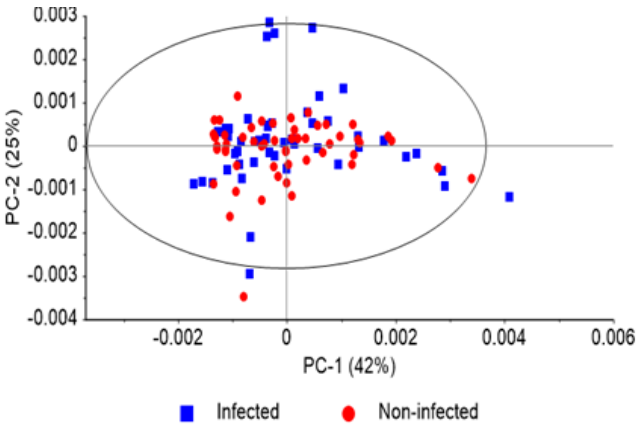

I

2nd Derivative + Atmospheric correction + UVN

J

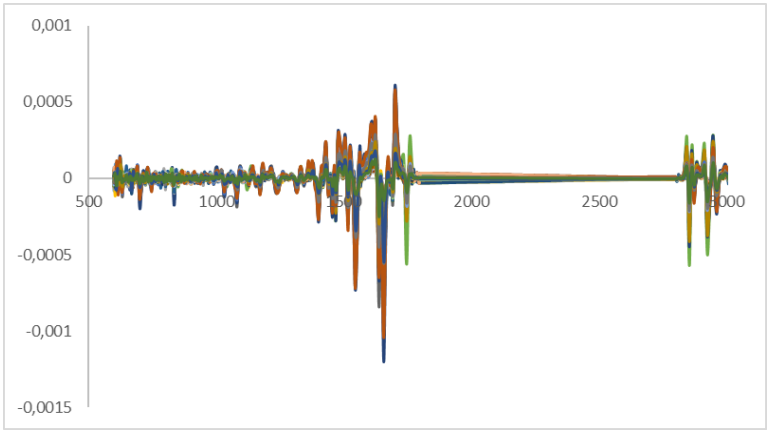

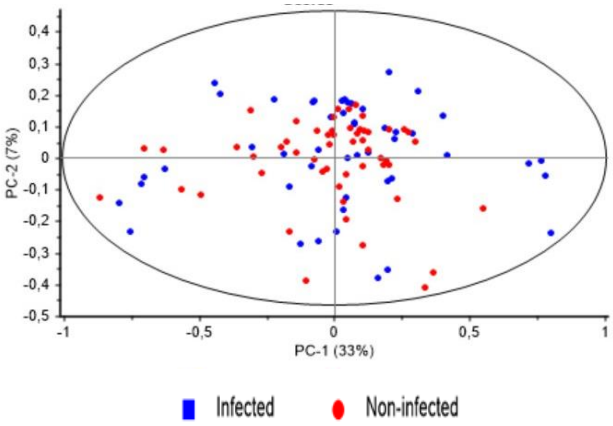

K

2nd Derivative + Atmospheric correction + Region of Interest

L

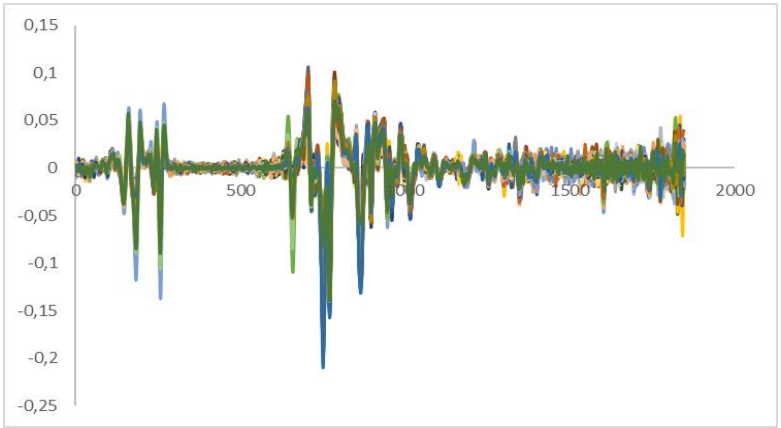

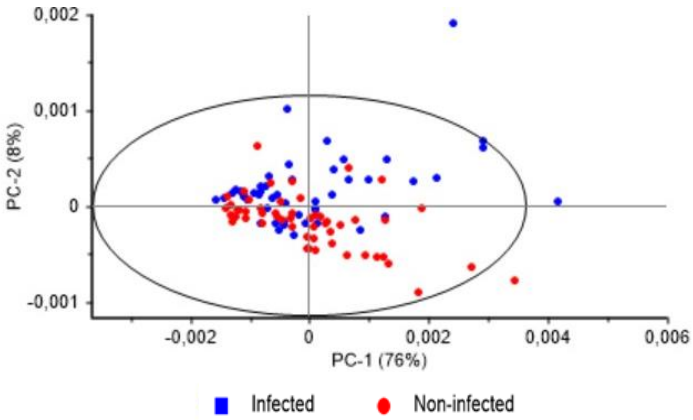

Figure 4.2.2 On the left side are spectra with different pre-processing methods, and on the right are the corresponding PCA between Infected with Bacteremia (Blue) and Not-Infected with Bacteremia (Red): (G&H) 2nd Derivative with atmospheric; (I&J) 2nd Derivative with UVN; (K&L) 2nd Derivative with region of interest 600-1800 cm^{-1} to 2800-3100 cm^{-1}.

2nd Derivative + Atmospheric correction + UVN + Region of Interest 600-1800 cm^{-1} + 2800-3100 cm^{-1}

M **N**

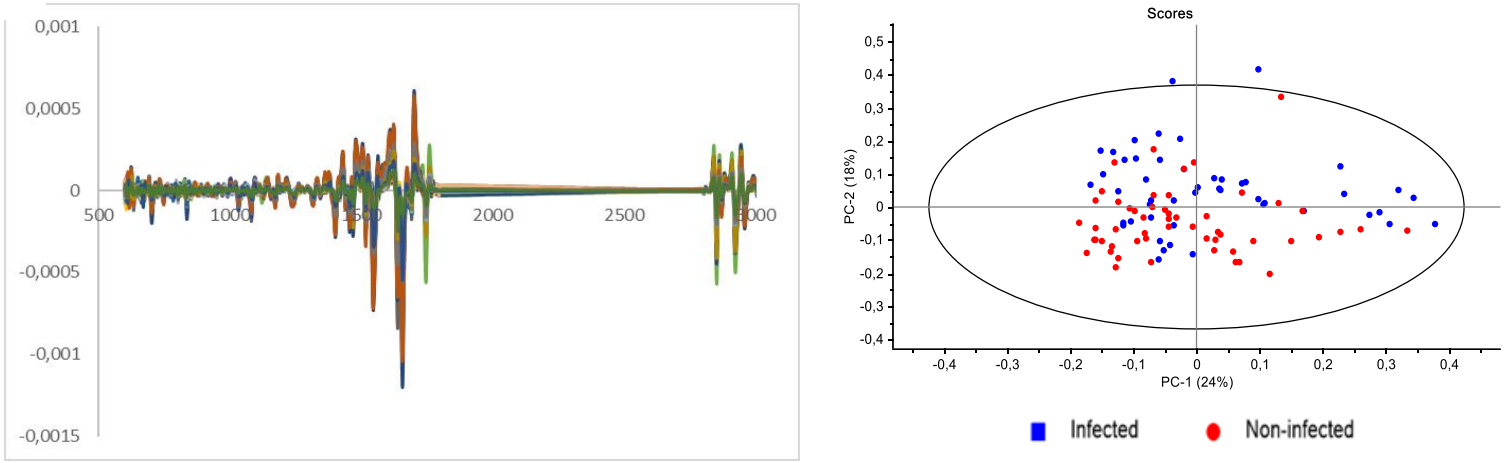

Figure 4.2.3 On the left side is spectra with different pre-processing method, and on the right are the corresponding PCA between Infected with Bacteremia (Blue) and Not-Infected with Bacteremia (Red): (M&N) 2nd Derivative with UVN and Regions of interest from 600-1800 cm^{-1} to 2800-3100 cm^{-1}

2nd Derivative + Atmospheric Correction

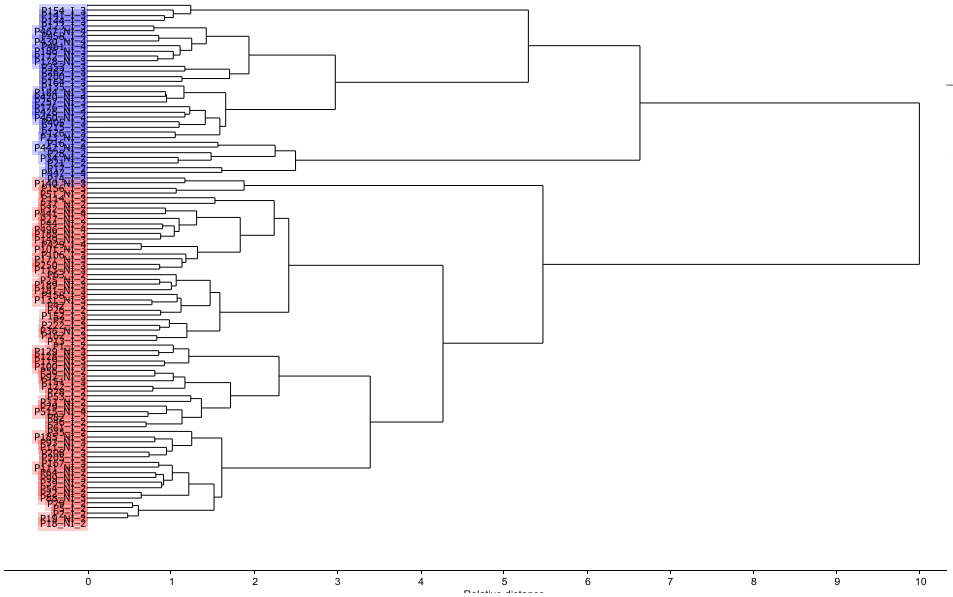

	Infected	*Non-Infected*
Cluster 1	20	14
Cluster 2	28	40

Figure 4.2.4 (A) Hierarchical clustering analysis with ATM and 2nd derivative using Ward's method with Squared Euclidean distance, (B) the corresponding confusion matrix.

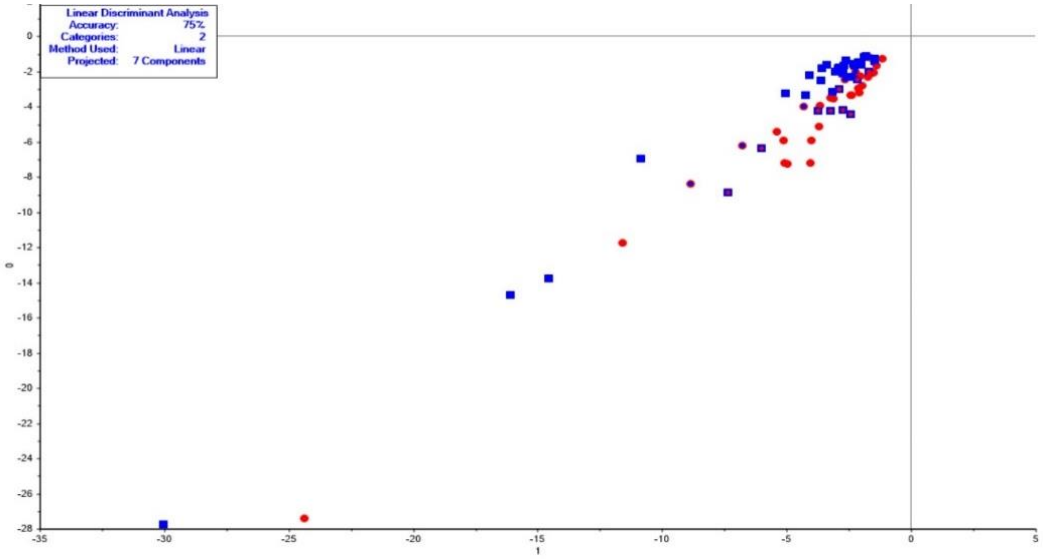

Atmospheric correction
+
Baseline

Accuracy: 75%
7 Components

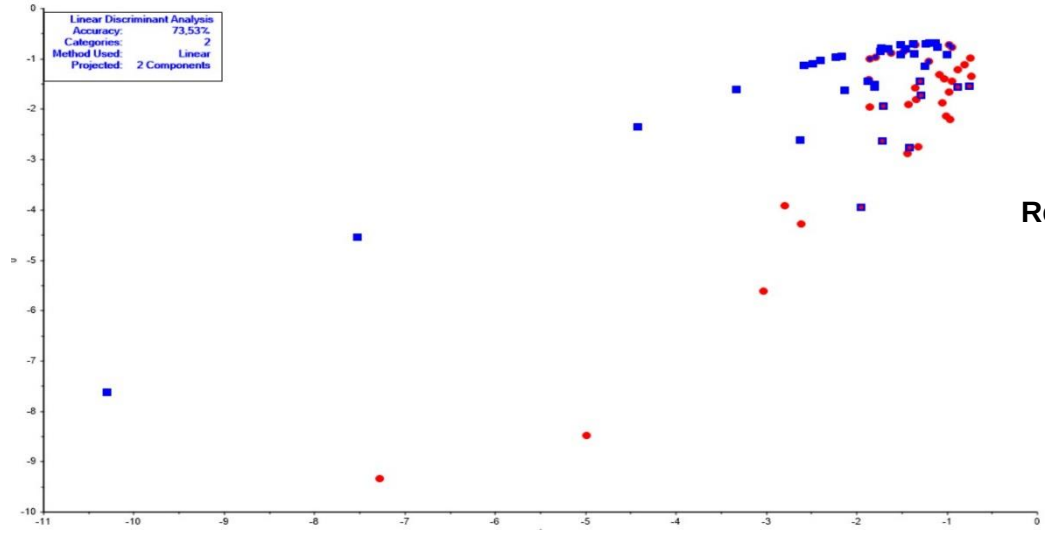

2nd Derivative
+
UVN
+
Regions of interest 600-1800 cm^{-1}
+ 2800-3100 cm^{-1}

Accuracy: 73.5%
2 Components

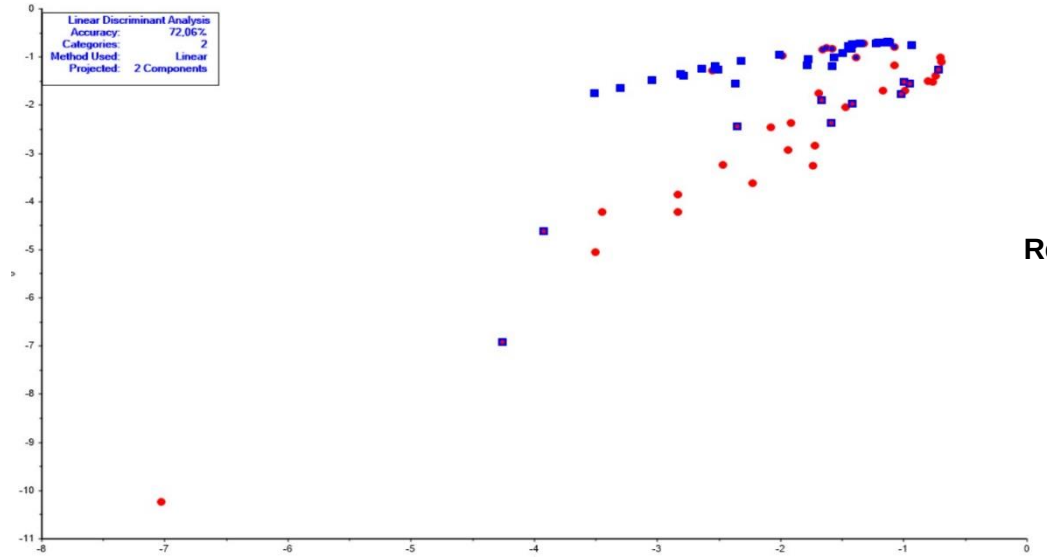

2nd Derivative
+
Atmospheric correction
+
Regions of interest 600-1800 cm^{-1}
+ 2800-3100 cm^{-1}

Accuracy: 72.1%
2 Components

Figure 4.2.5 Highest accuracies obtained in PCA-LDA with pre-processes. The calibration groups are represented as blue squares and circles, and the validation groups are shown as red squares and circles.

The best LDA analyses presented an accuracy percentage of 75%. Increasing the number of components didn't' lead to accuracy improvement.

Table 4.2.1 PCA-LDA results for "Bacteremia patients versus non-Bacteremia for each pre-processing while varying number of components from 2 to 7. Highest overall accuracy is presented in green.

Pre-processes	***Number of components***	***Accuracy (%)***
Atmospheric + Baseline Correction	2	58.8
	3	61.8
	4	60.3
	5	63.2
	6	64.7
	7	75.0
Atmospheric + Baseline correction + UVN	2	58.8
	3	58.9
	4	63.2
	5	69.1
	6	67.7
	7	69.1
Atmospheric correction + 2nd Derivative	2	57.4
	3	69.1
	4	72.1
	5	67.7
	6	69.1
	7	64.7
2nd Derivative + UVN	2	67.7
	3	69.1
	4	72.1
	5	67.7
	6	69.1
	7	64.7
2nd Derivative + Regions of interest 600-1800 cm^{-1} + 2800-3100 cm^{-1}	2	73.5
	3	67.7
	4	66.2
	5	67.7
	6	67.7
	7	64.7
2nd Derivative + UVN + Regions of interest 600-1800 cm^{-1} + 2800-3100 cm^{-1}	2	72.1
	3	72.1
	4	70.6
	5	70.6
	6	69.1
	7	69.1

4.3 Gram-Positive versus Gram-Negative

Results for FTIR spectroscopy discrimination for Gram-Positive versus Gram-Negative patients in the global sample is presented by PCA, HCA and PCA-LDA analysis for each pre-processing described before in **Chapter 3.4.** Once again, both PCA and HCA results showed a lack of efficiency for separation between the two groups. Visual presentation results obtained for both form of analyses is presented in **Figure 4.3.1**, **Figure 4.3.2**., **Figure 4.3.4**, **Figure 4.3.3**. The best PCA-LDA accuracies are shown in **Figure 4.3.6**

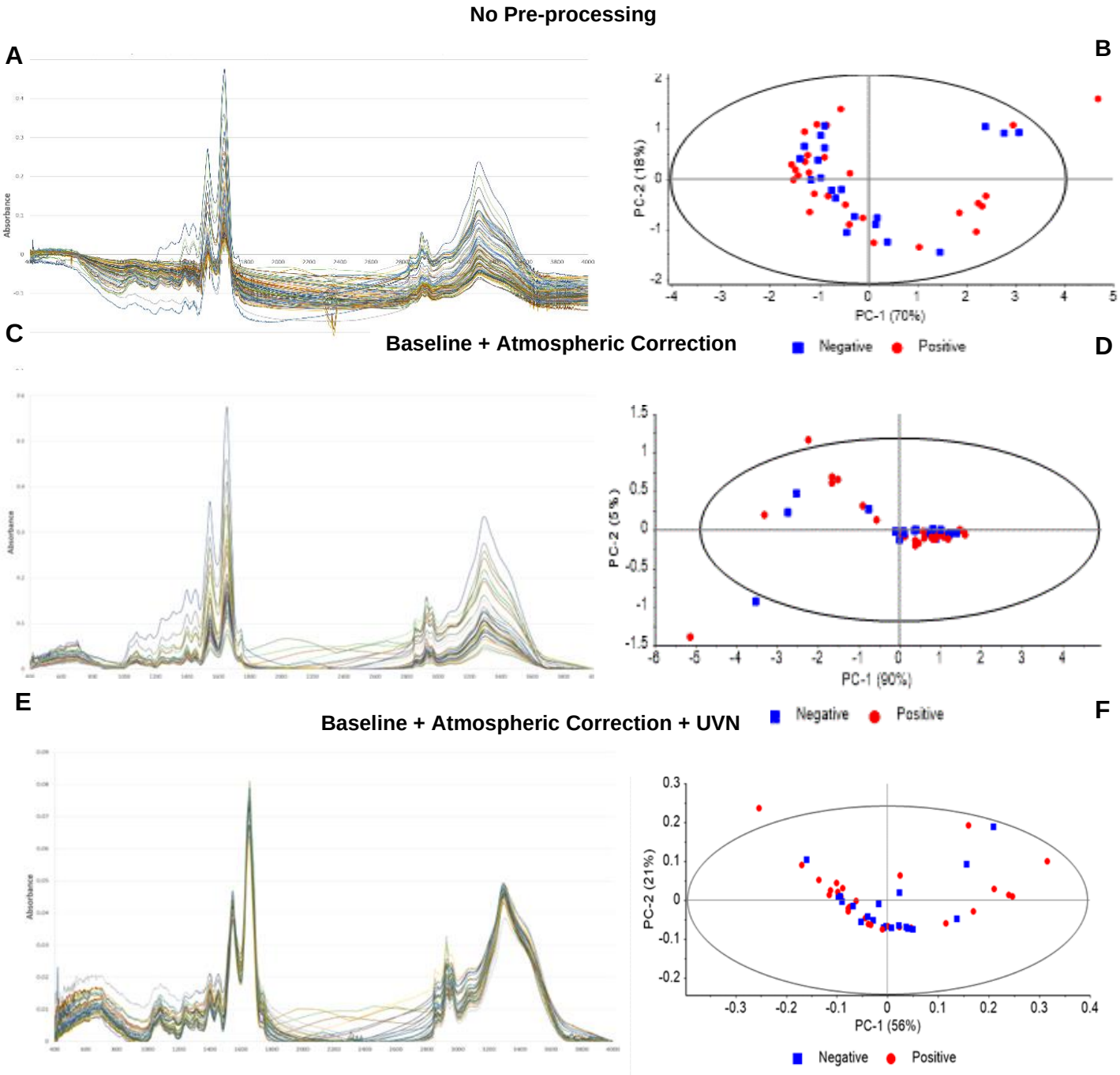

Figure 4.3.1 On the left side are spectra with different pre-processing methods, and on the right are the corresponding PCA between patients with Gram-Positive bacteremia (Blue) and patients with Gram-Negative bacteremia (Red): (A&B) Without pre-processing; (C&D) Atmospheric and Baseline correction; (E&F) Atmospheric and Baseline with UVN.

G

2nd Derivative + Atmospheric correction

H

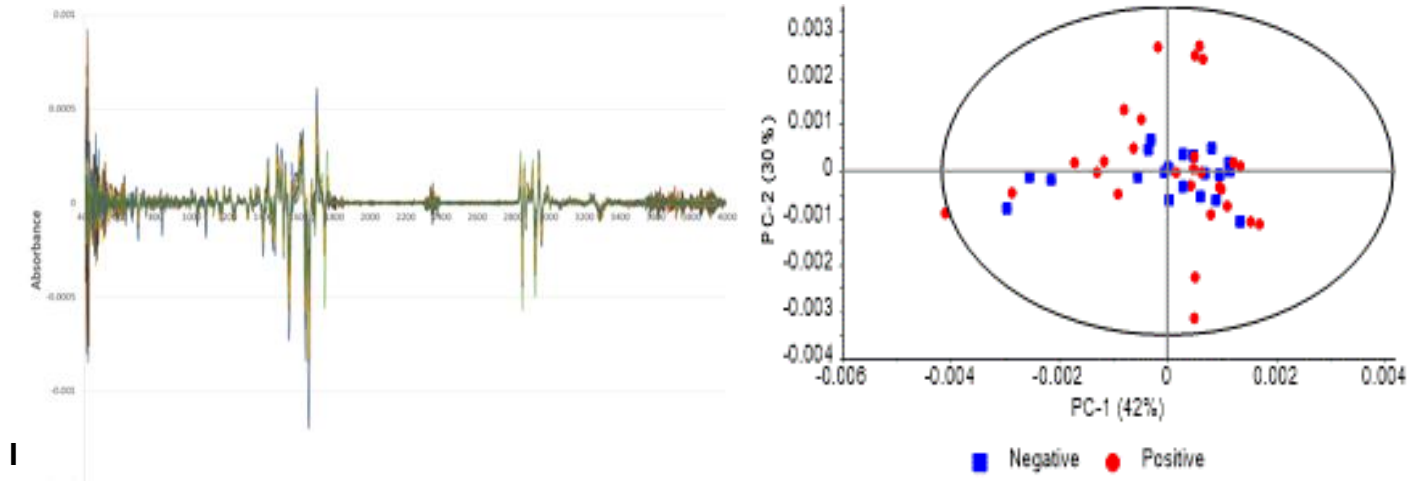

I

J

2nd Derivative + Atmospheric correction + UVN

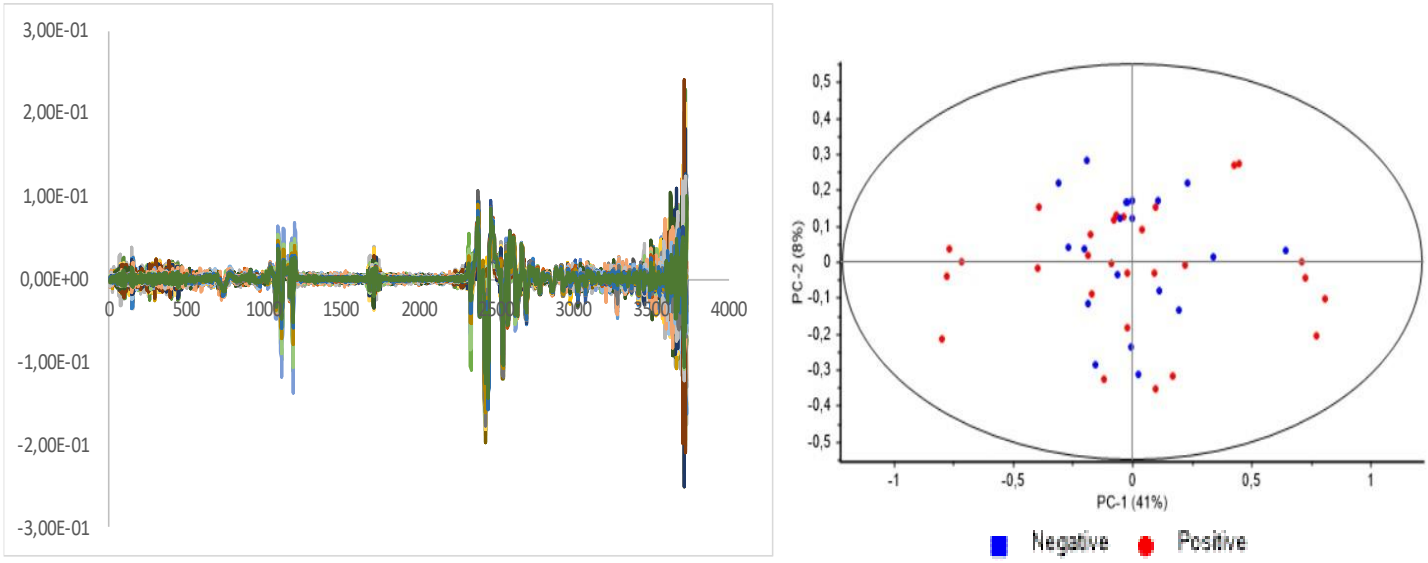

K

2nd Derivative + Atmospheric correction + Region of Interest 600-1800 cm^{-1} + 2800-3100 cm^{-1}

L

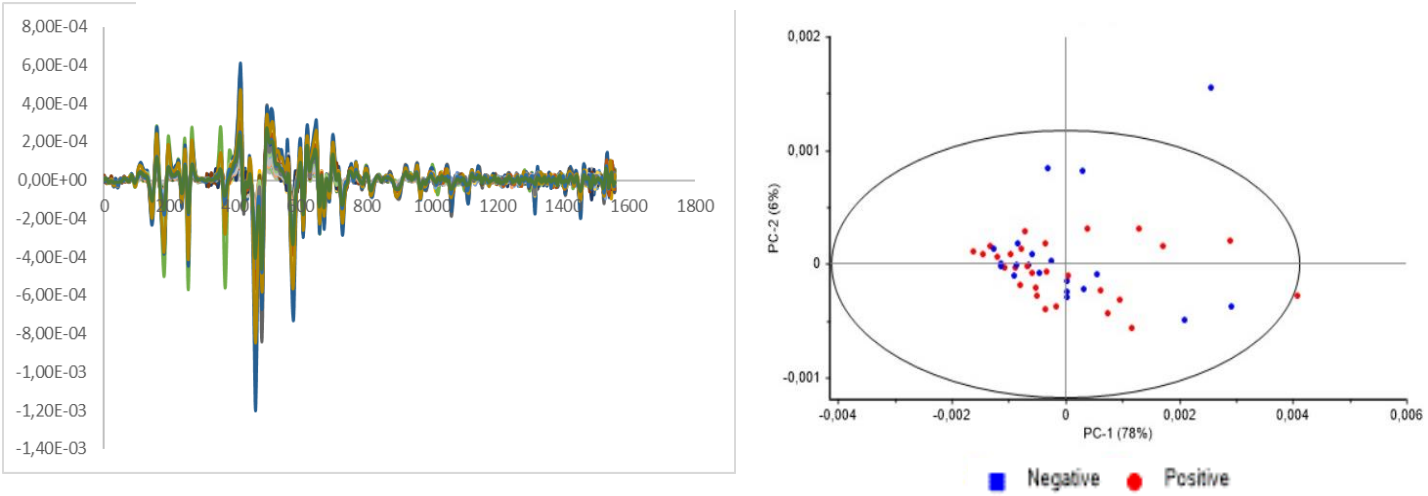

Figure 4.3.2 On the left side are spectra with different pre-processing methods, and on the right are the corresponding PCA between Infected with Gram-Negative (Blue) and Gram-Positive Bacteremia (Red): (G&H) 2nd Derivative with atmospheric; (I&J) 2nd Derivative with UVN; (K&L) 2nd Derivative with region of interest 600-1800 cm^{-1} to 2800-3100 cm^{-1}.

M **N**

2nd Derivative + Atmospheric correction + UVN + Region of Interest 600-1800 cm^{-1} + 2800-3100 cm^{-1}

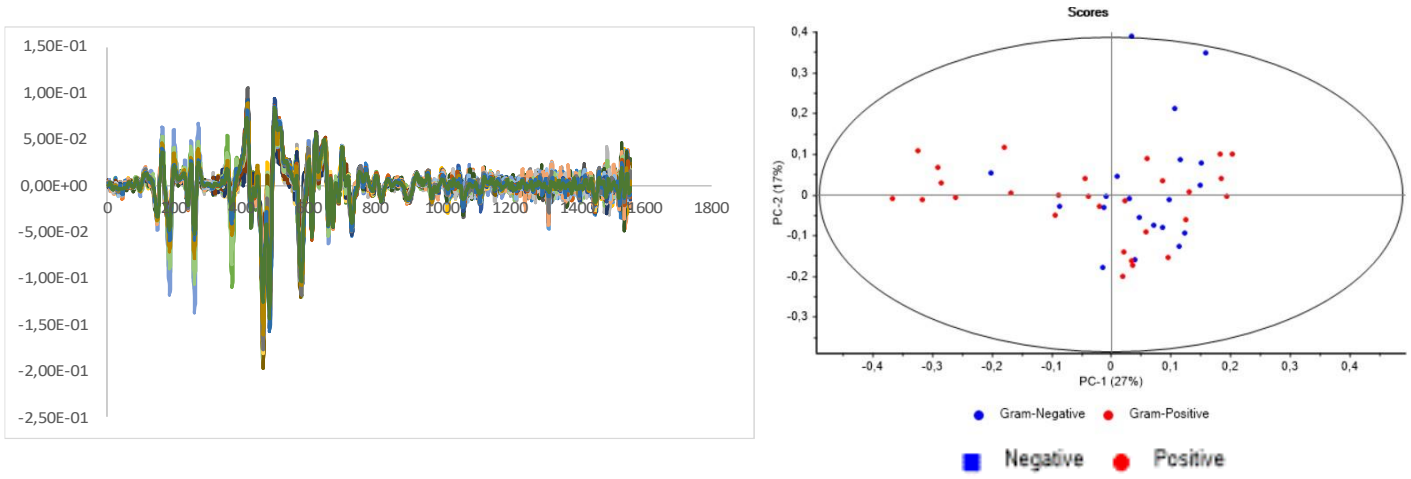

Figure 4.3.4 On the left side is spectra with 2nd Derivative plus atmospheric and UVN pre-processing, and on the right is it's the corresponding PCA between Gram-Negative Bacteremia (Blue) and Gram-Positive Bacteremia (Red): (M&N) 2nd Derivative with UVN and Regions of interest from 600-1800 cm^{-1} to 2800-3100 cm^{-1}

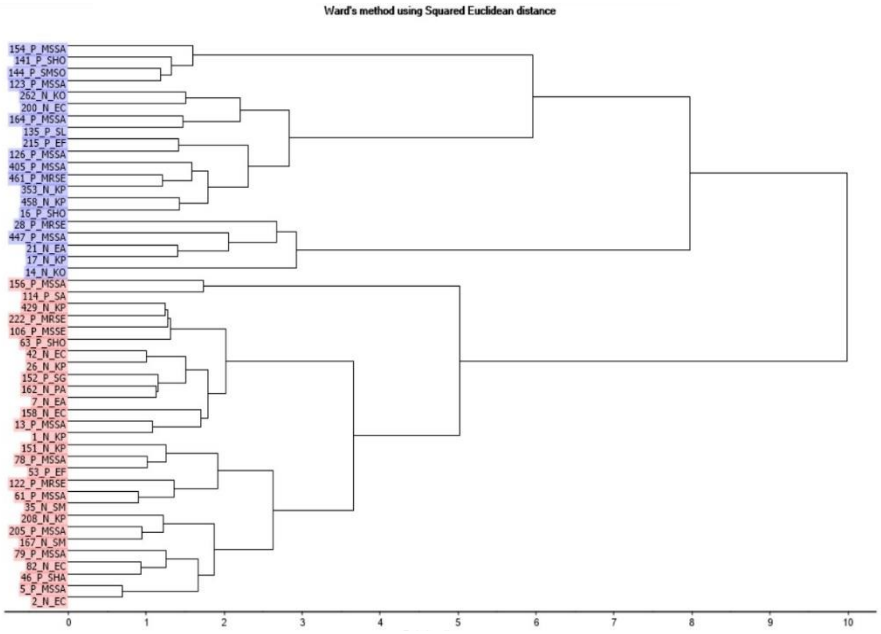

	Gram-Positive	*Gram-Negative*
Cluster 1	13	7
Cluster 2	15	13

Figure 4.3.3 (A) Hierarchical clustering analysis with Ward's with Squared Euclidean distance of 2nd Derivative with atmospheric correction (B), the corresponding confusion matrix.

PCA-LDA analyses, targeted towards Gram-Positive bacteremia patient's vs Gram-Negative bacteremia patients showed more promising results, seeing a reached efficiency of approximately 85%, reaching a noteworthy discrimination between the tested groups. (**Figure 4.3.5** and **Figure 4.3.6**) The best accuracy was obtained with 2nd Derivative with atmospheric correction, UVN and regions of interest (600-1800 cm^{-1} + 2800-3100 cm^{-1}) pre-process.

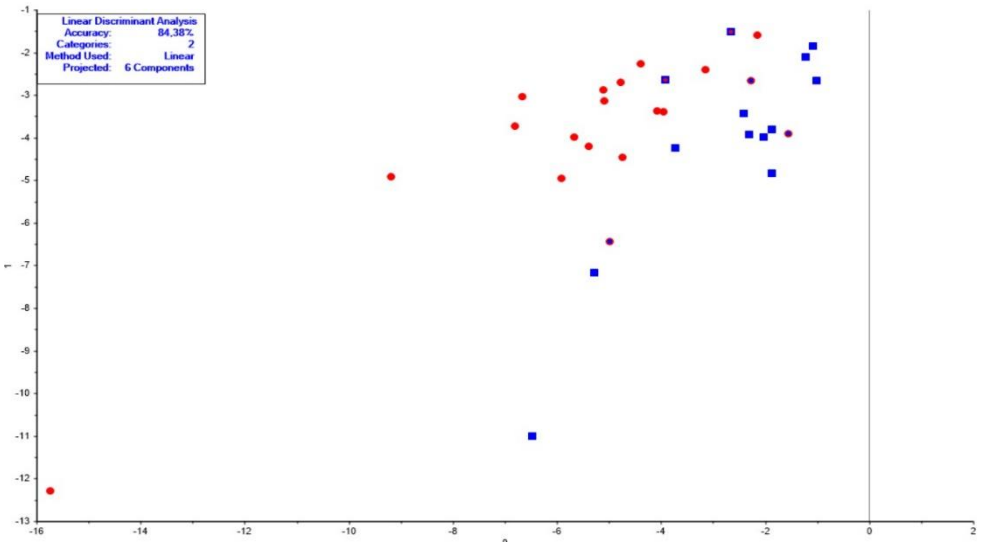

2nd Derivative
+
Atmospheric correction
+
Regions of interest
(600-1800 cm^{-1} + 2800-3100 cm^{-1})

Accuracy: 84.4%

6 Components

Figure 4.3.5 Highest accuracies obtained in PCA-LDA with pre-processes. The calibration groups are represented as blue squares and circles, and the validation groups are shown as red squares and circles.

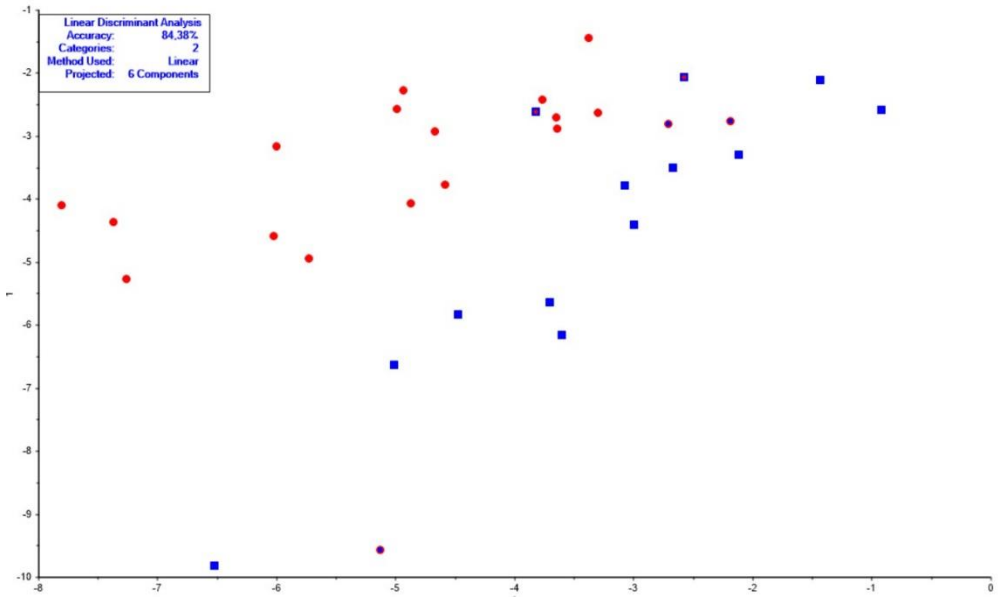

2nd Derivative
+
Atmospheric correction
+
UVN
+
Regions of interest
(600-1800 cm^{-1} + 2800-3100 cm^{-1})

Accuracy: 84.4%

6 Components

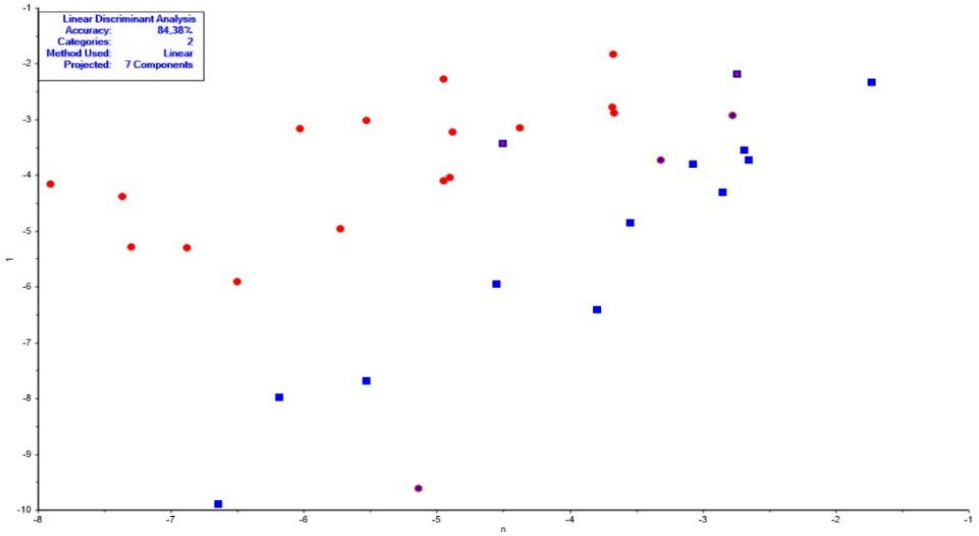

2nd Derivative
+
Atmospheric correction
+
UVN
+
Regions of interest
(600-1800 cm^{-1} + 2800-3100 cm^{-1})

Accuracy: 84.4%

7 Components

Figure 4.3.6 Highest accuracies obtained in PCA-LDA with pre-processes. The calibration groups are represented as blue squares and circles, and the validation groups are shown as red squares and circles.

It was observed that an incremented increase in components lead to higher discrimination efficiency. These results indicate that, contrary to what was previously observed in the Bacteremia versus non-Bacteremia analyses, FTIR spectroscopy discrimination can be a useful way to distinguish between bacterial gram-stains. By allowing for a faster determination of bacteria gram type, it promotes a more efficient use of antibiotics. Compiled PCA-LDA results can be observed in

.

Table 4.3.1 PCA-LDA results for "Gram-Positive patients versus Gram-Negative-Bacteremia for each pre-processing while varying number o*f* components from 2 to 7. Highest overall accuracy is presented in green.

Pre-processes	Number of components	Accuracy (%)
Atmospheric + Baseline Correction	2	56.3
	3	56.3
	4	65.6
	5	65.6
	6	59.4
	7	65.6
Atmospheric + Baseline correction + UVN	2	62.5
	3	56.3
	4	65.6
	5	68.8
	6	71.9
	7	75.0
Atmospheric correction + 2nd Derivative	2	59.4
	3	62.5
	4	65.6
	5	71.9
	6	71.9
	7	71.9
2nd Derivative + UVN	2	50.0
	3	59.4
	4	62.5
	5	62.5
	6	71.9
	7	71.9
2nd Derivative + Regions of interest 600-1800 cm^{-1} + 2800-3100 cm^{-1}	2	56.3
	3	68.8
	4	65.6
	5	71.9
	6	84.4
	7	81.3
2nd Derivative + UVN + Regions of interest 600-1800 cm^{-1} + 2800-3100 cm^{-1}	2	65.6
	3	65.6
	4	62.5
	5	81.3
	6	84.4
	7	84.4

In both studies, spectra PCA and HCA s weren't successful in discriminating groups. This result can be justified by the variability of the samples involved. Some patients also had positive cultures for urine and phlegm samples at the same time as the bacteremia was active. This leads to a multitude of other variables, and forms that certain patients' organisms may react, thus greatly altering the sample's composition. Once the sample is open to variability, metabolites and compounds will inevitably be altered, and samples may be incorrectly discriminated by FTIR spectroscopy.

Both patients' groups, Bacteremia and non-Bacteremia have this complication, thus complicating appropriate separation by PCA and HCA analyses. Another probable cause for PCA and HCA's lack of accuracy may be justified by the presence of multiple comorbidities across the global sample. While most patients tend to share comorbidities such as HTA, and *Diabetes mellitus*, other comorbidities among the sample may act as significant factor for sample composition due to their pro-inflammatory states (cancers, transplants).

LDA results on the other hand showed interesting results in both target studies, with the best accuracy being achieved in the discrimination of Gram stains. On contrary to PCA assays, that try to determine the axis with the highest variance possible, LDA assays aim to identify the best axis for best class segregation. This may lead to a better sample discrimination than the determined in PCAs. On average, the best LDA results seemed to have been obtained with the 2nd Derivative + UVN + Regions of interest 600-1800 cm^{-1} + 2800-3100 cm^{-1} pre-processing.

While an accuracy of 75% of Bacteremia identification may be a positive result, the determined accuracy of 84% for gram-stain separation in the 2nd Derivative with atmospheric correction and UVN (regions 600-1800 cm^{-1} + 2800-3100 cm^{-1}) is a sign that FTIR based discrimination may be a viable way to correctly discriminate Gram-stains. With this knowledge, antibiotic therapy may be selected faster upon infection detection, leading to a more effective, rapid treatment of active bacteremia.

5 Final Remarks and Future Work

FTIR spectroscopy has exponentially increased in popularity for a multitude of different types of analyses throughout the years. While its interest specifically for discrimination of bacteremia or gram-staining has been lesser explored, it still showed promising results. In this study, spectra PCA and HCA didn't provide the discrimination of the data-pattern, most probably due to the sample high diversity concerning e.g., comorbidities and co-infection The samples from patients with a higher diversity pathophysiological state could most probably be counteracted with a higher dimension of the studied population. Despite that, it was observed that discrimination accuracy improved with pre-processing techniques, like performing second derivative plus atmospheric correction

On the other hand, supervised methods, such as LDA, allowed sample discrimination in both studies. With an accuracy of 75% for bacteremia discrimination and the bacteria gram classification with an accuracy of 85%. This achievement is of extreme value, since it shows a great opportunity for improvement on the current bacteria strain identification, enabling a more precise antibiotic treatment.

In the future, with improvement of this study in mind, it would be useful to have a larger patient's sample, a deeper information concerning for the patient clinical variables, such as comorbidities and therapies.

6 References

1. Vincent JL, Sakr Y, Singer M, Martin-Loeches I, MacHado FR, Marshall JC, et al. Prevalence and Outcomes of Infection among Patients in Intensive Care Units in 2017. JAMA - J Am Med Assoc. 2020;323(15):1478–87.

2. Suleyman G, Fadel RA, Malette KM, Hammond C, Abdulla H, Entz A, et al. Clinical Characteristics and Morbidity Associated With Coronavirus Disease 2019 in a Series of Patients in Metropolitan Detroit. JAMA Netw open. 2020;3(6):e2012270.

3. Maki G, Zervos M. Health Care-Acquired Infections in Low- and Middle-Income Countries and the Role of Infection Prevention and Control. Infect Dis Clin North Am [Internet]. 2021 Sep;35(3):827–39. Available from: https://doi.org/10.1016/j.idc.2021.04.014

4. Anna S, Zahra F. Nosocomial Infections. In: StatPearls [Internet] [Internet]. Treasure Island (FL): StatPearls Publishing LLC; 2022. Available from: https://www.ncbi.nlm.nih.gov/books/NBK559312/?report=reader#_NBK559312_pubdet_

5. Khan HA, Baig FK, Mehboob R. Nosocomial infections: Epidemiology, prevention, control and surveillance. Asian Pac J Trop Biomed [Internet]. 2017;7(5):478–82. Available from: http://dx.doi.org/10.1016/j.apjtb.2017.01.019

6. Boni MF, Lemey P, Jiang X, Lam TTY, Perry BW, Castoe TA, et al. Evolutionary origins of the SARS-CoV-2 sarbecovirus lineage responsible for the COVID-19 pandemic. Nat Microbiol [Internet]. 2020;5(11):1408–17. Available from: http://dx.doi.org/10.1038/s41564-020-0771-4

7. Sugawara E, Nikaido H. Properties of AdeABC and AdeIJK efflux systems of Acinetobacter baumannii compared with those of the AcrAB-TolC system of Escherichia coli. Antimicrob Agents Chemother [Internet]. 2014 Dec [cited 2022 Aug 31];58(12):7250–7. Available from: https://www.who.int/emergencies/diseases/novel-coronavirus-2019/technical-guidance/naming-the-coronavirus-disease-(covid-2019)-and-the-virus-that-causes-it

8. Hageman JR. The coronavirus disease 2019 (COVID-19). Pediatr Ann. 2020;49(3):e99–100.

9. AJMC. A Timeline of COVID-19 Vaccine Developments in 2021 [Internet]. Ajmc. 2021 [cited 2022 Sep 1]. p. 1–15. Available from: https://www.ajmc.com/view/a-timeline-of-covid-19-vaccine-developments-in-2021

10. Kang N, Kim B. The effects of border shutdowns on the spread of COVID-19. J Prev Med Public Heal. 2020;53(5):293–301.

11. WHO Contributors. Impact of COVID-19 on people's livelihoods, their health and our food systems [Internet]. World Health Organization. 2022. Available from: https://www.who.int/news/item/13-10-2020-impact-of-covid-19-on-people%27s-livelihoods-their-health-and-our-food-systems#:~:text=The economic and social disruption,the end of the year.%3E

12. Eythorsson E, Runolfsdottir HL, Ingvarsson RF, Sigurdsson MI, Palsson R. Rate of SARS-CoV-2 Reinfection during an Omicron Wave in Iceland. JAMA Netw Open [Internet]. 2022 Aug 3;5(8):E2225320. Available from: https://jamanetwork.com/journals/jamanetworkopen/fullarticle/2794886

13. Liu Y, Yu Y, Zhao Y, He D. Reduction in the infection fatality rate of Omicron variant compared with previous variants in South Africa. Int J Infect Dis [Internet]. 2022;120:146–9. Available from: https://doi.org/10.1016/j.ijid.2022.04.029

14. THOMPSON SA. How Long Will a Vaccine Really Take? New York Times [Internet]. 2020;4–5. Available from: https://search.ebscohost.com/login.aspx?direct=true&db=n5h&AN=143028962&site=ehost-live

15. Sugawara E, Nikaido H. Properties of AdeABC and AdeIJK efflux systems of Acinetobacter baumannii compared with those of the AcrAB-TolC system of Escherichia coli. Antimicrob Agents Chemother [Internet]. 2014 Dec;58(12):7250–7. Available from: https://www.ajmc.com/view/a-timeline-of-covid-19-vaccine-developments-for-the-second-half-of-2021

16. Moghadas SM, Vilches TN, Zhang K, Wells CR, Shoukat A, Singer BH, et al. The Impact of Vaccination on Coronavirus Disease 2019 (COVID-19) Outbreaks in the United States. Clin Infect Dis [Internet]. 2021 Dec 16;73(12):2257–64. Available from: https://academic.oup.com/cid/article/73/12/2257/6124429

17. World Health Organization. COVID-19 Weekly Epidemiological Update. World Heal Organ [Internet]. 2022;(June):1–33. Available from: https://www.who.int/publications/m/item/covid-19-weekly-epidemiological-update

18. Yang Y, Peng F, Wang R, Guan K, Jiang T, Xu G, et al. The Deadly Coronaviruses: The 2003 SARS Pandemic and The 2020 Novel Coronavirus Epidemic in China , The Company' s Public News and Information. J Autoimmun [Internet].

2020;109(January):102487. Available from: https://www.sciencedirect.com/science/article/pii/S0896841120300470?via%3Dihub

19. O'Leary VB, Ovsepian SV. Severe Acute Respiratory Syndrome Coronavirus 2 (SARS-CoV-2). Trends Genet. 2020;36(11):892–3.

20. Sodeifian F, Nikfarjam M, Kian N, Mohamed K, Rezaei N. The role of type I interferon in the treatment of COVID-19. J Med Virol. 2022;94(1):63–81.

21. Ni W, Yang X, Yang D, Bao J, Li R, Xiao Y, et al. Role of angiotensin-converting enzyme 2 (ACE2) in COVID-19. Crit Care [Internet]. 2020 Dec 13;24(1):422. Available from: https://ccforum.biomedcentral.com/articles/10.1186/s13054-020-03120-0

22. Vellas C, Delobel P, De Souto Barreto P, Izopet J. COVID-19, Virology and Geroscience: A Perspective. J Nutr Heal Aging [Internet]. 2020 Jul 18;24(7):685–91. Available from: https://link.springer.com/10.1007/s12603-020-1416-2

23. Alimohamadi Y, Sepandi M, Taghdir M, Hosamirudsari H. Determine the most common clinical symptoms in COVID-19 patients: A systematic review and meta-analysis. J Prev Med Hyg [Internet]. 2020 Sep;61(3):E304–12. Available from: http://www.ncbi.nlm.nih.gov/pubmed/33150219

24. Yong SJ. Long COVID or post-COVID-19 syndrome: putative pathophysiology, risk factors, and treatments. Infect Dis (Auckl) [Internet]. 2021 Oct 3;53(10):737–54. Available from: https://doi.org/10.1080/23744235.2021.1924397

25. Adab P, Haroon S, O'Hara ME, Jordan RE. Comorbidities and covid-19. BMJ [Internet]. 2022 Jun 15;1431. Available from: https://www.bmj.com/lookup/doi/10.1136/bmj.o1431

26. Sanyaolu A, Okorie C, Marinkovic A, Patidar R. Comorbilidad y su impacto en pacientes con COVID-19. SN Compr Clin Med. 2020;2:1069–76.

27. Johnson M. Wuhan 2019 Novel Coronavirus - 2019-nCoV. Mater Methods [Internet]. 2020 Jan 23;10(JANUARY):1–5. Available from: https://www.labome.com/method/Wuhan-2019-Novel-Coronavirus-2019-nCoV.html

28. National Institutes of Health. Treatment Guidelines Panel. Coronavirus Disease 2019 (COVID-19). Nih [Internet]. 2021;2019:1–243. Available from: https://www.covid19treatmentguidelines.nih.gov/.%0Ahttps://www.covid19treatmentguidelines.nih.gov/

29. Haft JW, Atluri P, Ailawadi G, Engelman DT, Grant MC, Hassan A, et al. Adult Cardiac

Surgery During the COVID-19 Pandemic: A Tiered Patient Triage Guidance Statement. Ann Thorac Surg. 2020;110(2):697–700.

30. Hadjadj J, Yatim N, Barnabei L, Corneau A, Boussier J, Smith N, et al. Impaired type I interferon activity and inflammatory responses in severe COVID-19 patients. Science (80-) [Internet]. 2020 Aug 7;369(6504):718–24. Available from: http://www.ncbi.nlm.nih.gov/pubmed/32661059

31. Schreiber G. The Role of Type I Interferons in the Pathogenesis and Treatment of COVID-19. Front Immunol. 2020;11(September):8–10.

32. Eskandarian Boroujeni M, Sekrecka A, Antonczyk A, Hassani S, Sekrecki M, Nowicka H, et al. Dysregulated Interferon Response and Immune Hyperactivation in Severe COVID-19: Targeting STATs as a Novel Therapeutic Strategy. Front Immunol [Internet]. 2022;13(May):888897. Available from: http://www.ncbi.nlm.nih.gov/pubmed/35663932

33. Biffi S, Di Bella S, Scaravilli V, Peri AM, Grasselli G, Alagna L, et al. Infections during extracorporeal membrane oxygenation: epidemiology, risk factors, pathogenesis and prevention. Int J Antimicrob Agents [Internet]. 2017;50(1):9–16. Available from: http://dx.doi.org/10.1016/j.ijantimicag.2017.02.025

34. Holmes CL, Anderson MT, Mobley HLT. Pathogenesis of Gram-Negative Bacteremia. 2021;(March):1–27.

35. Lachhab Z, Frikh M, Maleb A, Kasouati J, Doghmi N, Ben Lahlou Y, et al. Bacteraemia in Intensive Care Unit: Clinical, Bacteriological, and Prognostic Prospective Study. Can J Infect Dis Med Microbiol [Internet]. 2017;2017:1–9. Available from: https://www.hindawi.com/journals/cjidmm/2017/4082938/

36. Tsalik EL, Jones D, Nicholson B, Waring L, Liesenfeld O, Park LP, et al. Multiplex PCR to diagnose bloodstream infections in patients admitted from the emergency department with sepsis. J Clin Microbiol [Internet]. 2010 Jan;48(1):26–33. Available from: https://journals.asm.org/doi/10.1128/JCM.01447-09

37. Font MD, Thyagarajan B, Khanna AK. Sepsis and Septic Shock – Basics of diagnosis, pathophysiology and clinical decision making. Med Clin North Am. 2020;104(4):573–85.

38. Jansen GJ, Mooibroek M, Idema J, Harmsen HJM, Welling GW, Degener JE. Rapid identification of bacteria in blood cultures by using fluorescently labeled oligonucleotide probes. J Clin Microbiol. 2000;38(2):814–7.

39. Kollef MH, Shorr AF, Bassetti M, Timsit JF, Micek ST, Michelson AP, et al. Timing of antibiotic therapy in the ICU. Crit Care [Internet]. 2021;25(1):1–10. Available from: https://doi.org/10.1186/s13054-021-03787-z

40. Agaba P, Tumukunde J, Tindimwebwa JVB, Kwizera A. Nosocomial bacterial infections and their antimicrobial susceptibility patterns among patients in Ugandan intensive care units: A cross sectional study. BMC Res Notes [Internet]. 2017 Jul 28;10(1):349. Available from: http://bmcresnotes.biomedcentral.com/articles/10.1186/s13104-017-2695-5

41. Khan HA, Ahmad A, Mehboob R. Nosocomial infections and their control strategies. Asian Pac J Trop Biomed [Internet]. 2015;5(7):509–14. Available from: http://dx.doi.org/10.1016/j.apjtb.2015.05.001

42. Dadi NCT, Radochová B, Vargová J, Bujdáková H. Impact of Healthcare-Associated Infections Connected to Medical Devices—An Update. Microorganisms [Internet]. 2021 Nov 11;9(11):2332. Available from: https://www.mdpi.com/2076-2607/9/11/2332

43. Percival SL, Suleman L, Vuotto C, Donelli G. Healthcare-Associated infections, medical devices and biofilms: Risk, tolerance and control. J Med Microbiol. 2015;64(4):323–34.

44. Norbury W, Herndon DN, Tanksley J, Jeschke MG, Finnerty CC. Infection in burns. Surg Infect (Larchmt) [Internet]. 2016 Apr;17(2):250–5. Available from: https://www.liebertpub.com/doi/10.1089/sur.2013.134

45. Alqahtani A, Alamer E, Mir M, Alasmari A, Alshahrani MM, Asiri M, et al. Bacterial Coinfections Increase Mortality of Severely Ill COVID-19 Patients in Saudi Arabia. Int J Environ Res Public Health. 2022;19(4).

46. Shafran N, Shafran I, Ben-Zvi H, Sofer S, Sheena L, Krause I, et al. Secondary bacterial infection in COVID-19 patients is a stronger predictor for death compared to influenza patients. Sci Rep [Internet]. 2021;11(1):1–8. Available from: https://doi.org/10.1038/s41598-021-92220-0

47. Brusselaers N, Vogelaers D, Blot S. The rising problem of antimicrobial resistance in the intensive care unit. Ann Intensive Care [Internet]. 2011 Dec 23;1(1):47. Available from: http://www.annalsofintensivecare.com/content/1/1/47

48. Gransden WR. Antibiotic resistance. Nosocomial gram-negative infection. J Med Microbiol [Internet]. 1997 Jun 1 [cited 2022 Sep 17];46(6):436–9. Available from: https://www.who.int/news-room/fact-sheets/detail/antibiotic-resistance

49. Smith MA. Antibiotic Resistance. Nurs Clin North Am [Internet]. 2005 Mar [cited 2022 Sep 21];40(1):63–75. Available from: https://www.who.int/news-room/fact-sheets/detail/antibiotic-resistance

50. ABRAHAM EP. The Antibiotics. In: Comprehensive Biochemistry [Internet]. 1963. p. 181–224. Available from: https://linkinghub.elsevier.com/retrieve/pii/B9781483197111500223

51. Yoshimura J, Yamakawa K, Ohta Y, Nakamura K, Hashimoto H, Kawada M, et al. Effect of Gram Stain–Guided Initial Antibiotic Therapy on Clinical Response in Patients With Ventilator-Associated Pneumonia. JAMA Netw Open [Internet]. 2022 Apr 8;5(4):e226136. Available from: https://jamanetwork.com/journals/jamanetworkopen/fullarticle/2790906

52. Alexandraki I, Palacio C. Gram-negative versus Gram-positive bacteremia: What is more alarmin(g)? Crit Care. 2010;14(3).

53. Zhu Q, Zhu M, Li C, Li L, Guo M, Yang Z, et al. Epidemiology and microbiology of Gram-negative bloodstream infections in a tertiary-care hospital in Beijing, China: a 9-year retrospective study. Expert Rev Anti Infect Ther [Internet]. 2021 Jun 3;19(6):769–76. Available from: http://www.ncbi.nlm.nih.gov/pubmed/33187451

54. Luzzaro F, Viganò EF, Fossati D, Grossi A, Sala A, Sturla C, et al. Prevalence and drug susceptibility of pathogens causing bloodstream infections in northern Italy: A two-year study in 16 hospitals. Eur J Clin Microbiol Infect Dis. 2002;21(12):849–55.

55. Pathak A, Agrawal A. Evolution of C-reactive protein. Front Immunol. 2019;10(APR).

56. Sproston NR, Ashworth JJ. Role of C-Reactive Protein at Sites of Inflammation and Infection. Front Immunol [Internet]. 2018 Apr 13;9(APR):1–11. Available from: http://journal.frontiersin.org/article/10.3389/fimmu.2018.00754/full

57. Pepys MB, Hirschfield GM. C-reactive protein: a critical update. J Clin Invest [Internet]. 2003 Jul 15;112(2):299–299. Available from: http://www.jci.org/articles/view/18921C1

58. Pierrakos C, Velissaris D, Bisdorff M, Marshall JC, Vincent JL. Biomarkers of sepsis: Time for a reappraisal. Crit Care. 2020;24(1):1–15.

59. Khourssaji M, Chapelle V, Evenepoel A, Belkhir L, Yombi JC, van Dievoet MA, et al. A biological profile for diagnosis and outcome of COVID-19 patients. Clin Chem Lab Med. 2020;58(12):2141–50.

60. Silvestre J, Rebanda J, Lourenço C, Póvoa P. Diagnostic accuracy of C-reactive

protein and procalcitonin in the early detection of infection after elective colorectal surgery - a pilot study. BMC Infect Dis. 2014;14(1):1–8.

61. Eschborn S, Weitkamp J-H. Procalcitonin versus C-reactive protein: review of kinetics and performance for diagnosis of neonatal sepsis. J Perinatol [Internet]. 2019 Jul 29;39(7):893–903. Available from: http://dx.doi.org/10.1038/s41372-019-0363-4

62. Fan S, Miller NS, Lee J, Remick DG. Crp Discussion. 2017;203–10.

63. Hertz FB, Ahlström MG, Bestle MH, Hein L, Mohr T, Lundgren JD, et al. Early Biomarker-Guided Prediction of Bloodstream Infection in Critically Ill Patients: C-Reactive Protein, Procalcitonin, and Leukocytes. Open Forum Infect Dis [Internet]. 2022 Oct 5;9(10):1–7. Available from: https://doi.org/10.1093/ofid/ofac467

64. Tanaka T, Narazaki M, Kishimoto T. IL-6 in Inflammation, Immunity, and Disease. 2014;6(Kishimoto 1989):1–16.

65. Scheller J, Chalaris A, Schmidt-Arras D, Rose-John S. The pro- and anti-inflammatory properties of the cytokine interleukin-6. Biochim Biophys Acta - Mol Cell Res. 2011;1813(5):878–88.

66. Gabay C. Interleukin-6 and chronic inflammation. Arthritis Res Ther [Internet]. 2006;8 Suppl 2(SUPPL. 2):S3. Available from: http://www.ncbi.nlm.nih.gov/pubmed/16899107

67. Wu Y, Wang M, Zhu Y, Lin S. Serum interleukin-6 in the diagnosis of bacterial infection in cirrhotic patients. Medicine (Baltimore) [Internet]. 2016 Oct;95(41):e5127. Available from: https://journals.lww.com/00005792-201610110-00041

68. Aloisio E, Dolci A, Panteghini M. Procalcitonin: Between evidence and critical issues. Clin Chim Acta. 2019;496(May):7–12.

69. Paudel R, Dogra P, Montgomery-Yates AA, Yataco AC. Procalcitonin: A promising tool or just another overhyped test? Int J Med Sci. 2020;17(3):332–7.

70. Hoeboer SH, van der Geest PJ, Nieboer D, Groeneveld ABJ. The diagnostic accuracy of procalcitonin for bacteraemia: a systematic review and meta-analysis. Clin Microbiol Infect [Internet]. 2015 May;21(5):474–81. Available from: http://dx.doi.org/10.1016/j.cmi.2014.12.026

71. Daryapeyma A, Pedersen G, Laxdal E, Corbascio M, Johannessen HB, Aune S, et al. Neutrophil CD64 as a marker for postoperative infection: a pilot study. Eur J Vasc Endovasc Surg [Internet]. 2009 Jul;38(1):100–3. Available from: https://doi.org/10.1186/s13613-018-0479-2

72. de Jong E, de Lange DW, Beishuizen A, van de Ven PM, Girbes ARJ, Huisman A. Neutrophil CD64 expression as a longitudinal biomarker for severe disease and acute infection in critically ill patients. Int J Lab Hematol. 2016;38(5):576–84.

73. Liang J, Xu J, You L, Yang G, Niu G, Pan H, et al. Neutrophil CD64: a potential biomarker for the diagnosis of infection in patients with haematological malignancies. Hematology [Internet]. 2021 Jan 1;26(1):970–5. Available from: https://www.tandfonline.com/doi/full/10.1080/16078454.2021.2003064

74. Yeh C-F, Wu C-C, Liu S-H, Chen K-F. Comparison of the accuracy of neutrophil CD64, procalcitonin, and C-reactive protein for sepsis identification: a systematic review and meta-analysis. Ann Intensive Care [Internet]. 2019;9(1):5. Available from: https://doi.org/10.1186/s13613-018-0479-2

75. Ahnach M, Zbiri S, Nejjari S, Ousti F, Elkettani C. C-reactive protein as an early predictor of COVID-19 severity. J Med Biochem. 2020;39(4):500–7.

76. Liu F, Li L, Xu M, Wu J, Luo D, Zhu Y, et al. Prognostic value of IL-6, CRP, and PCT in patients with COVID-19. J Clin Virol. 2020;7(January):0–5.

77. Bivona G, Agnello L, Ciaccio M. Biomarkers for Prognosis and Treatment Response in COVID-19 Patients. Ann Lab Med [Internet]. 2021 Nov 1;41(6):540–8. Available from: http://annlabmed.org/journal/view.html?doi=10.3343/alm.2021.41.6.540

78. Richter DC, Heininger A, Brenner T, Hochreiter M, Bernhard M, Briegel J, et al. Bacterial sepsis. Anaesthesist [Internet]. 2019 Feb;68(S1):40–62. Available from: http://link.springer.com/10.1007/s00101-017-0396-z

79. Lachhab Z, Frikh M, Maleb A, Kasouati J, Doghmi N, Ben Lahlou Y, et al. Bacteraemia in Intensive Care Unit: Clinical, Bacteriological, and Prognostic Prospective Study. Can J Infect Dis Med Microbiol [Internet]. 2017;2017:1–9. Available from: https://www.hindawi.com/journals/cjidmm/2017/4082938/

80. Bassetti M, Righi E, Carnelutti A. Bloodstream infections in the Intensive Care Unit. Virulence [Internet]. 2016;7(3):267–79. Available from: http://dx.doi.org/10.1080/21505594.2015.1134072

81. Mostaço-Guidolin LB, Murakami LS, Nomizo A, Bachmann L. Fourier transform infrared spectroscopy of skin cancer cells and tissues. Appl Spectrosc Rev. 2009;44(5):438–55.

82. Movasaghi Z, Rehman S, Rehman IU. Fourier transform infrared (FTIR) spectroscopy of biological tissues. Appl Spectrosc Rev. 2008;43(2):134–79.

83. Bruker. Guide to Infrared Spectroscopy [Internet]. Spectroscopy Basics. 2021 [cited 2022 Sep 18]. Available from: https://www.bruker.com/en/products-and-solutions/infrared-and-raman/ft-ir-routine-spectrometer/what-is-ft-ir-spectroscopy.html

84. Araújo RAD. Impact of Epigallocatechin-3-gallate (EGCG) on the molecular profile of plasma and serum. 2019;(December). Available from: http://hdl.handle.net/10400.21/13286

85. Saxton R, McDougal OM. Whey protein powder analysis by mid-infrared spectroscopy. Foods. 2021;10(5):1–18.

86. Sahu RK, Argov S, Salman A, Huleihel M, Grossman N, Hammody Z, et al. Characteristic absorbance of nucleic acids in the Mid-IR region as possible common biomarkers for diagnosis of malignancy. Technol Cancer Res Treat. 2004;3(6):629–38.

87. Mohamed MA, Jaafar J, Ismail AF, Othman MHD, Rahman MA. Fourier Transform Infrared (FTIR) Spectroscopy. In: Membrane Characterization [Internet]. Elsevier; 2017. p. 3–29. Available from: http://dx.doi.org/10.1016/B978-0-444-63776-5.00001-2

88. WiredSense. The Michelson Interferometer - A Laser Lab Alignment Guide [Internet]. WiredSense. 2018 [cited 2022 Sep 21]. Available from: https://www.wiredsense.com/tutorials/the-michelson-interferometer-a-laser-lab-alignment-guide

89. Michelson T. Interferometers 2 . Michelson interferometer : theory. :1–18.

90. Chua SC, Chong FK, Ul Mustafa MR, Mohamed Kutty SR, Sujarwo W, Abdul Malek M, et al. Microwave radiation-induced grafting of 2-methacryloyloxyethyl trimethyl ammonium chloride onto lentil extract (LE-g-DMC) as an emerging high-performance plant-based grafted coagulant. Sci Rep [Internet]. 2020 Dec 3;10(1):3959. Available from: http://www.nature.com/articles/s41598-020-60119-x

91. Palm S. FT-IR: Fourier Transform Infrared Spectroscopy [Internet]. 2020 [cited 2022 Sep 25]. Available from: https://niom.no/ft-ir-fourier-transform-infrared-spectroscopy/

92. CHIHARA G. Clinical Applications of Infrared Spectroscopy. J Spectrosc Soc Japan [Internet]. 1961;9(4):181–96. Available from: http://www.jstage.jst.go.jp/article/bunkou1951/9/4/9_4_181/_article/-char/ja/

93. Wang-Wang JH, Bordoy AE, Martró E, Quesada MD, Pérez-Vázquez M, Guerrero-Murillo M, et al. Evaluation of Fourier Transform Infrared Spectroscopy as a First-Line Typing Tool for the Identification of Extended-Spectrum β-Lactamase-Producing

Klebsiella pneumoniae Outbreaks in the Hospital Setting. Front Microbiol. 2022;13(June).

94. Silva L, Rodrigues C, Lira A, Leão M, Mota M, Lopes P, et al. Fourier transform infrared (FT-IR) spectroscopy typing: a real-time analysis of an outbreak by carbapenem-resistant Klebsiella pneumoniae. Eur J Clin Microbiol Infect Dis. 2020;39(12):2471–5.

95. Novais Â, Freitas AR, Rodrigues C, Peixe L. Fourier transform infrared spectroscopy: unlocking fundamentals and prospects for bacterial strain typing. Eur J Clin Microbiol Infect Dis. 2019;38(3):427–48.

96. Vogt S, Löffler K, Dinkelacker AG, Bader B, Autenrieth IB, Peter S, et al. Fourier-Transform Infrared (FTIR) Spectroscopy for Typing of Clinical Enterobacter cloacae Complex Isolates. Front Microbiol. 2019;10(November):1–11.

97. Preisner O, Lopes JA, Guiomar R, MacHado J, Menezes JC. Fourier transform infrared (FT-IR) spectroscopy in bacteriology: Towards a reference method for bacteria discrimination. Anal Bioanal Chem. 2007;387(5):1739–48.

98. Deidda F, Bozzi Cionci N, Cordovana M, Campedelli I, Fracchetti F, Di Gioia D, et al. Bifidobacteria Strain Typing by Fourier Transform Infrared Spectroscopy. Front Microbiol [Internet]. 2021 Sep 13;12(September):1–10. Available from: https://www.frontiersin.org/articles/10.3389/fmicb.2021.692975/full

99. Nuttall FQ. Body mass index: Obesity, BMI, and health: A critical review. Nutr Today. 2015;50(3):117–28.

100. Yu Z, Kastenmüller G, He Y, Belcredi P, Möller G, Prehn C, et al. Differences between human plasma and serum metabolite profiles. PLoS One. 2011;6(7):1–6.

101. Autsavapromporn N, Klunklin P, Chitapanarux I, Jaikang C, Chewaskulyong B, Sripan P, et al. A Potential Serum Biomarker for Screening Lung Cancer Risk in High Level Environmental Radon Areas: A Pilot Study. Life [Internet]. 2021 Nov 21;11(11):1273. Available from: https://www.mdpi.com/2075-1729/11/11/1273

102. Debes J, Romagnoli P, Prieto J, Arrese M, Mattos A, Boonstra A. Serum Biomarkers for the Prediction of Hepatocellular Carcinoma. Cancers (Basel) [Internet]. 2021 Apr 2;13(7):1681. Available from: https://www.mdpi.com/2072-6694/13/7/1681

103. Camo Software AS. The Unscrambler X user manual. Oslo; 2014.